**ORIGINAL PAPER**

# Wire electrochemical micromachining of nitinol shape memory alloy using different electrolytes

**Naresh Besekar[1] · B. Bhattacharyya[1]**

## Abstract

Nitinol shape memory alloy (SMA) is one of the toughest and difficult to cut advanced smart material. Also, the properties of the material should not be affected during machining operations. Wire electrochemical machining (WECM) was created to address these issues as a result of technological innovation and the necessity for high aspect ratio products. This paper explains the effect of different aqueous solution of electrolytes, i.e., NaBr, NaCl, and $NaNO_3$ on nitinol dimensional and surface characteristics by microgroove fabrications during WECM. Further, in order to improve machining performance, the machining has been carried out with mixed and ozonated mixed conditions of $NaCl + NaNO_3$ electrolytes, and the quality of machined microgrooves is examined for surface topography, dimensional precision, and homogeneity. The best electrolyte, i.e., $NaCl + NaNO_3$ has been further used in combination with EDTA (ethylenedinitrilotetraacetic acid disodium salt dehydrate) complexing agent under non-ozonated and ozonated conditions and resulted in improved surface finish and dimensional features of the microfeatures by expeditiously removing sludge and dissolved products and increasing the efficacy of dissolution than other electrolytic conditions. The average groove width of 105.86 μm, mean depth of 264.6 μm, average surface roughness of 0.1346 μm, homogeneous microslit of average width of 106.40 μm, and average surface roughness (Ra) of 0.1261 μm have been obtained at 5 V pulse voltage and 1.4 μm/s wire feed rate with ozonated aqueous 0.2 M $NaCl + 0.2$ M $NaNO_3$ mixed with 0.2 M EDTA.

**Keywords** Wire electrochemical machining · Electrolytes · Micromachining · Nitinol · Shape memory alloy

## Introduction

Electrochemical micromachining (EMM) has made a remarkable impact in the area of advanced micro manufacturing through fabrication of various microproducts that are successfully utilized in various micro engineering applications. EMM has diversified, and their operational capability has been increased by the introduction of different features to exploit its potential in the area of submicron and nano range fabrication. Wire electrochemical machining (WECM) is a relatively recent technique that can effortlessly produce complex 3D high aspect ratio microfeatures on a variety of tough to process materials without experiencing any

heat stress, burr formation, or tool wear [1]. Nitinol is a special material that can change shape when heated; as a result, it is referred to as a shape memory alloy. However, nitinol's beneficial properties, such its high ductility, work hardening, and temperature sensitivity, can make it challenging to use in conventional fabrication techniques. Among these challenges include tool wear, the development of many burrs, and micro cracks. Furthermore, the material's shape memory effect may be reduced or eliminated by the mechanical and thermal stresses. These difficulties make it challenging to machine nitinol, severely restricting its use in a variety of sectors. Alternative machining procedures were investigated in an effort to overcome the difficulties nitinol presented during standard machining techniques. These include, among others, water jet machining, electrical discharge machining, and laser machining. But these unconventional methods frequently have unwanted effects, like the development of a recast layer, an increase in residual stress, and higher machining temperatures [2]. High corrosion resistance, biocompatibility, elasticity, resilience, and

✉ Naresh Besekar
  nareshwbesekar@gmail.com

  B. Bhattacharyya
  bb13@rediffmail.com

1 Production Engineering Department, Jadavpur University,
  Kolkata 700032, India

a constant transition temperature are just a few of this material's remarkable qualities. Due to these qualities, nitinol is perfect for usage in a variety of fields, such as biomedicine, transportation, aviation, robotics, and microelectronics [3]. Li et al. presented an improved flushing technique for microgroove production using phosphoric acid and ethanol as the electrolyte [4]. Takashi et al. investigated the effects of pulse voltage on the basic characteristics of nitinol using LiCl-ethanol electrolyte solution. Wide etching patterns were seen and the surfaces were often rough [5]. Ao et al. proposed a micro electrochemical milling technique for nitinol processing that makes use of an ethanol-added ethylene glycol-NaCl electrolyte. Numerous investigations were carried out to enhance the machining of nitinol [6]. Sethi et al. used various neutral electrolytes for ECMM to investigate the dissolving behavior of nitinol and showed that there was still potential for improvement in surface quality and accuracy of the machining [7]. Lee et al. used short-pulse ECM for microgroove machining of nitinol and discovered that surface roughness improved with an acid electrolyte [8]. Guo et al. compared milling to EDM of nitinol and focused on the surface properties. Large burrs form when milling at a high feed rate; however, EDM produces surfaces without burrs and produces thick white layers as a result of heat that may be decreased with an EDM finish trim cut [9]. Ma et al. developed a method of confine etchant-layer in order to create microstructures on the nitinol alloy's surface and produce a distinct 3D pattern [10]. Saxena et al. reviewed that the different authors used a variety of techniques to increase the accuracy of the microfeatures created using ECMM. Among the few techniques that produced precise microfeatures were process parameter optimizations, side wall insulation of the micro tool, and creative micro tool design [11]. Lopes et al. investigated several parameters for electrolytic polishing of nitinol wire in both the elastic and shape memory phases using a 3.5 mol/L methanolic $H_2SO_4$ electrolyte solution at 20 °C [12].

MouliPrasanth et al. used EMM to assess the 3D surface roughness of nitinol and discovered that composite electrolytes provided the highest surface integrity [13]. Hang et al. demonstrated the capabilities of this technique to create components without any processing flaws by reducing WEDM surfaces to obtain smooth surfaces without a recast layer on Rene 88DT for aerospace applications [14]. Lee et al. used short pulse ECM to create nitinol micro-grooves in order to investigate the machining characteristics. In order to avoid the precipitation of Ni $(OH)_2$ while using solely $NaNO_2$ as the electrolyte, 1.5 M $NaNO_2$ and 0.1 M $Na_2C_4H_4O_6$ were used as the electrolytes to dissolve the SMA [15]. Sharma et al. have proven WECM to be a workable approach for micromachining [16]. Besekar et al. concluded that the PTFE tube insulation approach was the most effective as compared to other several insulation techniques

for decreasing stray current and overcut during wire electrochemical machining [17]. Sethi et al. used a combined citric acid + $NaNO_3$ electrolyte to study the EC dissolution of a WC-Co micro tool in WECM and produced a higher surface finish [18]. Xu et al. investigated that the fabricated microfeature surface roughness was influenced by mass transport conditions [19]. In their experimental study, Tak et al. discovered that adding EDTA to a solution minimizes the production of titanium oxides on the machined surface of the holes during pulse-ECMM of titanium alloy, which in turn tends to reduce the stray currents. Improved titanium alloy machining results in less overcutting of holes when electrolyte solutions containing EDTA are used [20]. Jiang et al. suggested the suspension of $B_4C$ particles in the electrolyte for vibration-assisted wire electrochemical micromachining. The $NaNO_3$ electrolyte was mixed with a suspension of $B_4C$ particles in response to the experimental findings, and the electrolytic products that had accumulated on the wire cathode's surface were successfully eliminated by the low-frequency vibration of the wire cathode [21]. According to Kalaimathi et al., the TWECM process settings and the ozonated aqueous NaCl electrolyte both affect the machining performances for Monel 400 alloys, namely, the material removal rate (MRR) and surface roughness (Ra). The removal of oxide and sludge deposits from the specimen surface is what causes the MRR in the ozonated aqueous NaCl electrolyte to rise by 3 to 90% [22]. Anasane et al. experimentally found that the NaBr electrolyte has been best suited for electrochemical micromachining of titanium alloy in terms of dimensional accuracy and surface characteristics [23]. Sethi et al. carried out investigation for precise fabrication of nitinol microchannels at different inter electrode gaps with pulse frequency and micro tool rotational speed through ECMM [24]. Besekar et al. investigated the effect of different wire electrochemical machining process parameters during micromachining of nitinol SMA and characterized the machined microfeatures for changes in chemical compositions and surface topography by comparing it with non-machined surface utilizing field emission scanning electron microscopy (FESEM), energy dispersive X-ray spectroscopy (EDX), and X-ray diffraction (XRD) tests [25].

This paper describes the fabrication of microgrooves and microslits of nitinol shape memory alloy using wire electrochemical machining (WECM), a material that is well suited for use in biomedical and MEMS applications. The goal of this work was to investigate the precise methodology for creating microgrooves on nitinol utilizing different neutral aqueous electrolytes, i.e., NaBr, NaCl, and $NaNO_3$ electrolytes for dimensional and surface characteristics analysis with different electrolyte concentrations. Further, non-ozonated and ozonated mixed electrolytes with and without addition of EDTA (ethylenedinitrilotetraacetic acid disodium salt dehydrate) as complexing agent, i.e., NaCl + $NaNO_3$
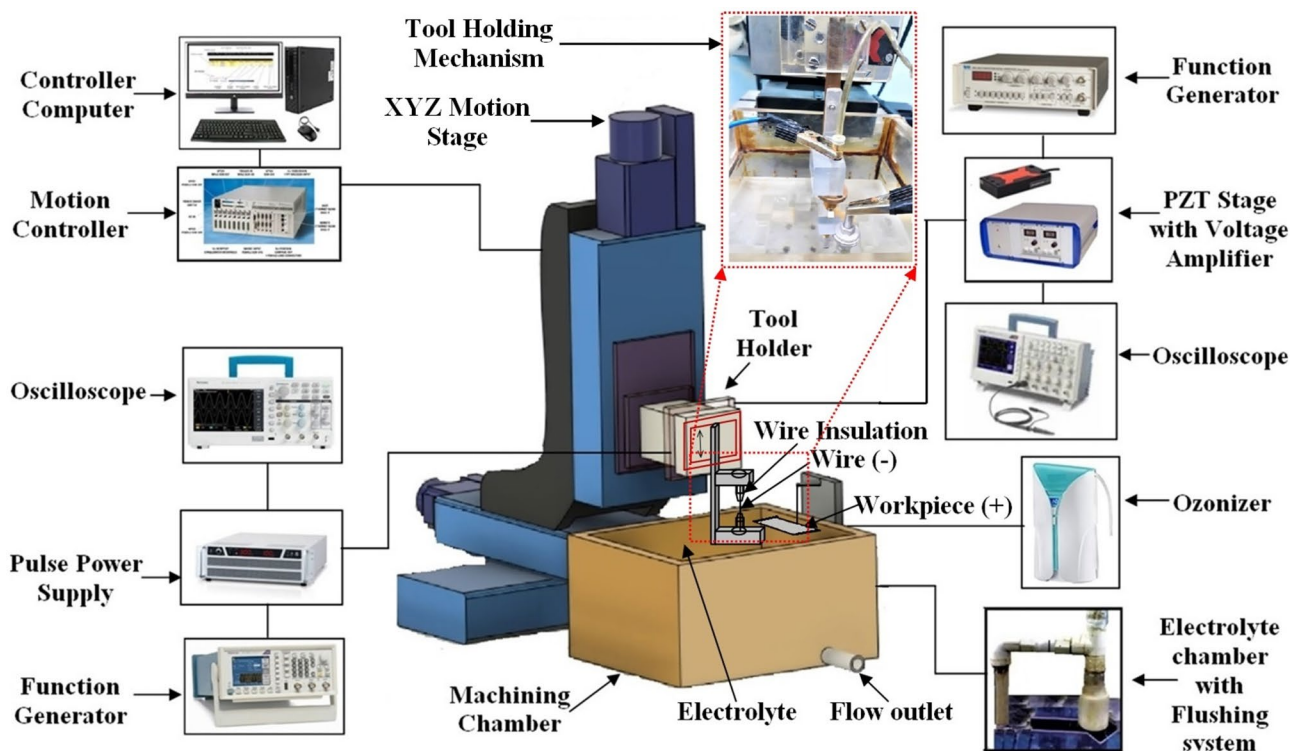
**Fig. 1** Schematics of in-house-developed experimental setup

and NaCl + NaNO$_3$ + EDTA electrolyte have been used to improve homogeneity and surface integrity of fabricated micro-features and confirm with FESEM, EDS analysis, and measurement of surface profile for 3D profiles and average roughness (Ra) values.

## Materials and methods

### Work materials

In this study, 1-mm-thick commercially-available nitinol sheets of 15 mm × 15 mm dimensions (consisting of 56 atomic % Ni and 44 atomic % Ti and martensite below 80 °C, heat treatments for 30 min at 550–750 °C, and water quench at 80 to 10 °C for activation) were employed and used after undergoing ultrasonic cleaning in acetone to eliminate any dirt or impurities. Also, 200-μm nitinol sheet has been used for microslit fabrication. A cylindrical tungsten wire with a diameter of 50 μm was used as electrode. From the previous literature, it was recommended that NaBr (lab grade 99% AR) is suitable for titanium, and NaNO$_3$ (lab grade 99% AR) and NaCl (lab grade 99.5% purity) electrolytes produced in distilled water (pH-5.97, 99.9% purity) are appropriate for efficient dissolution of nitinol; and hence, the same was used for the present experiments. Also, it has been observed that the addition of suitable complexing agents is proven to be the best solution for improvement in the surface finish of microfeatures; therefore, EDTA is also used in the experimentations in combination with most suitable electrolytes for machining of nitinol among all these electrolyte solutions. Also, ozone generator with ozone output of 250 mg/h has been used for experimentation in ozonated electrolytes during WECM of nitinol.

### Experimental setup

The microfeature fabrication was carried out using in-house-developed vibration-assisted axial nozzle jet flow WECM experimental setup utilizing different components and subsystems for specific applications. The schematics of developed WECM setup, as depicted in Fig. 1, are outfitted with three linear high precision stages for the *X*, *Y*, and *Z*-axis. The Newport XPS QS motion controller software is used to control the 0.1-μm/step resolution stepper motors. The machining chamber mounted and fixed on breadboard of the stage and the wire holder is mounted on *Z*-axis stage and feed motion. The power supply is producing maximum current at different pulse voltages up to 4 A. The function generator and oscilloscope have been connected with the power supply to vary different energy input parameter and monitor the waveforms during machining. The machining

chamber has enough ozone in it created using ozonator. For controlling appropriate flow, a suitable axial electrolyte flow system has been created, and fresh electrolytes have been passed axially through the small nozzles near the machining zone combined with the small frequency and amplitude PZT vibrations for efficient flushing. The wire has been held vertically straight with proper tension with insulation on non-machined area to avoid effect of stray current and can be reusable for numbers of experiments.

The ozone has been produced using ozonizer in the machining chamber for improvement in the performance of WECM process. A pulsed DC power supply (Matsusada DOA75) is employed to keep the polarity consistent during WECM. The power supply is readily available and offers a voltage range of $-75$ to $+75$ V, a current rating of up to 4 A, and a maximum power output of 300W. A pulse generator device is used to produce the necessary types of pulses. To determine the pulse's nature and to keep track of the machining conditions, a function generator (Tektronix AFG1022) is utilized. A tool holding device fabricated from acrylic material is developed and attached to the Z-axis of stage. The machine is featured with continuity setting for microsparks recognition using Tektronix TBS 2000 series digital oscilloscope. The PZT stage has been connected with the tool for providing axial vibration with small amplitude and frequency with the help of voltage amplifier through function generator and monitoring the pulses with oscilloscope.

## Methodology

To evaluate the effect of different electrolytes, i.e., NaBr, NaCl, and NaNO$_3$ with and without ozonated conditions and addition of complexing agent, i.e., EDTA on the accuracy, homogeneity, and surface integrity of microfeatures, experiments were conducted using wide range of electrolyte concentrations with constant pulse voltage, feed rate, and duty ratio for analyzing material removal rate and surface roughness. This article outlines each procedure and action that must be followed to complete the required sets of tests. To begin the experiment and get the electrolyte flowing via the gap between the electrodes, place the workpiece on the work holding platform. Mount the wire electrode in the tool holder and feed it towards the workpiece to ensure the just in contact condition, which is tested for with a continuity tester. All of the machining settings have been changed in line with the anticipated experimental planning and provided feed rates in the stage controller for the forward movement of the wire electrode towards the workpiece. The investigations on ozonated electrolytes in case of nitinol dissolving during WECM deserve more investigation. Table 1 displays the machining parameters for each process parameter and the experimental ranges that they were employed in. The wire is positioned on an XYZ translation stage that has an overall

**Table 1** Machining parameters

| Working condition | Value |
| --- | --- |
| Workpiece material | Nitinol SMA |
| Workpiece thickness | 1 mm, 200 μm |
| Wire electrode material | Tungsten |
| Diameter of wire electrode | Ø50 μm |
| Applied pulse voltage | 5 V |
| Wire feed rate | 1.4 μm/s |
| Duty ratio | 50% |
| Voltage pulse frequency | 250 kHz |
| Time of each experiment | 3 min |
| Electrolyte flow rate | 35 lph |
| IEG | 50 μm |
| PZT tool vibration frequency | 50 Hz |
| PZT tool vibration amplitude | 12.54 μm |
| Ozone output from ozone generator | 250 mg/h |

travel distance of 100 mm for each axis and a resolution of 0.1 μm. For the purpose of creating linear micro grooves on nitinol SMA, the workpiece and wire were maintained in a vertically straight posture.

The arrangement was kept steady, while the wire electrode was supplied linearly. Both the workpiece and the fixture were submerged in the electrolyte bath. All the experimentations have been carried out using this in-house developed experimental setup for 3 min using different combinations of electrolytes and its concentration. The aqueous neutral NaBr, NaNO$_3$, and NaCl electrolyte solutions in the range of 0.2 to 0.4 M concentration have been used for all the experimentations. The mixtures of these electrolytes with 0.2 M concentration have been used considering the best results in terms of surface finish and dimensional characteristics. Further, 0.2 M EDTA has been added to the mixture of 0.2 M NaCl and 0.2 M NaNO$_3$ under ozonated and non-ozonated conditions for improvement in the surface finish and machining accuracy.

## Measurements

Surface roughness and dimensional characteristics have been assessed at each step of varied circumstances of process parameters during WECM of machined micro grooves for each operating conditions in order to examine experimental results and improve the quality of the micro machined product. During tests, the oscilloscope has been utilized to track various pulse power characteristics. The studies have also been conducted using a multimeter, a stereo zoom microscope, an optical camera, a microscope, among other tools. The output responses were measured and machined microgrooves parameters were carefully examined under an optical microscope Leica, Germany, and CCI (coherent correlation interferometer) profilometer made by Taylor Hobson for
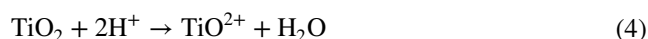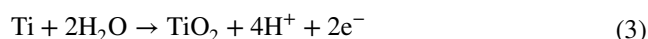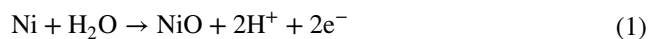
their dimensions, i.e., width and depth and surface roughness and 3D profile of the microgrooves. Further, in-depth analysis and characterization of the fabricated microfeatures have been carried out for these electrolytes using FESEM and EDS for changes in the surface characteristics and chemical compositions during WECM on nitinol shape memory alloy. The elemental composition of the fresh nitinol sample used for fabrication of microgrooves and microslits has been presented herewith through SEM, EDS, and 3D surface profile as shown in Fig. 2. The non-machined nitinol SMA has elemental composition mass% of 1.36 carbon C, 1.87 oxygen O, 48.65 titanium Ti, and 48.12 nickel Ni depicted through EDX and average surface roughness (Sa) of 0.7393 μm measured through CCI profilometer. Carbon peaks are the results of oxidation as well as organic impurities in the electrolytes. It probably comes from organic impurities in electrolytes as well as environmental conditions even from air.

## Results and discussion

### Effect of neutral electrolytes on the accuracy and surface finish

When compared to the anodic dissolution of the other metals in WECM, nitinol is a particularly difficult to machine. Because there is a thin coating of passive $TiO_2$ on the surface,

it offers good resistance to anodic dissolution. Surface oxidation under atmospheric circumstances is one of the main issues with nitinol electrochemical dissolution. Nitinol develops a passive oxide deposit on its surface and its partial dissolution when exposed to an oxygen-containing solution. Nitinol creates an oxide layer consisting of $TiO_2$ and NiO in aqueous solution and its partial dissolution, according to the equations below [26].

$$Ni + H_2O \rightarrow NiO + 2H^+ + 2e^- \tag{1}$$

$$NiO + 2H^+ \rightarrow Ni^{2+} + H_2O \tag{2}$$

$$Ti + 2H_2O \rightarrow TiO_2 + 4H^+ + 2e^- \tag{3}$$

$$TiO_2 + 2H^+ \rightarrow TiO^{2+} + H_2O \tag{4}$$

According to certain investigations, the oxide film is dual in nature, with $TiO_2$ layer on top and interacting with the NiO sublayer. Ni dissolves through pores in the thinnest $TiO_2$ layer due to the substantially reduced resistance of these NiO sublayers to pitting. Ti(IV) is more sensitive to pH than Ni(II), as it undergoes deep hydrolysis even in acidic solutions. Ti(IV) aqueous chemistry is extremely complex but can be briefly formulated as follows: $Ti^{4+}$ never exists in aqueous solutions; at pH below 3, predominating
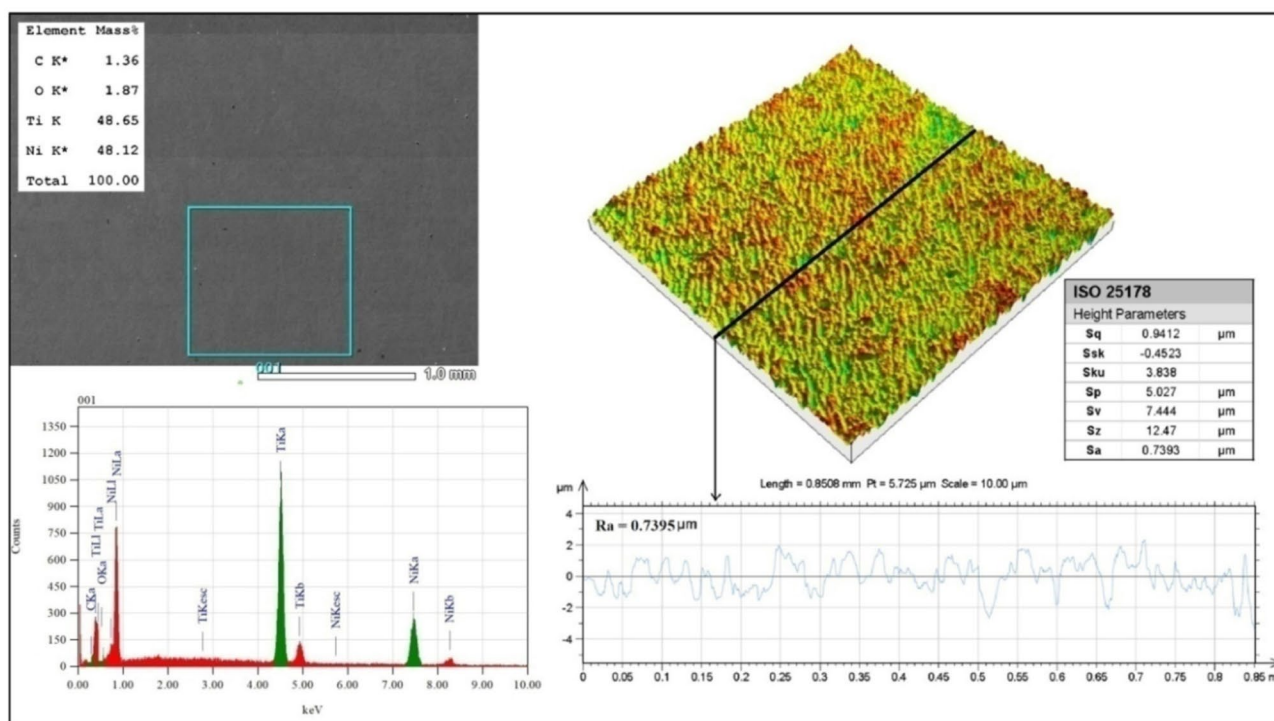


**Fig. 2** Elemental composition and 3D surface roughness profile of non-machined nitinol sample

specie is $[Ti(OH)_2]^{2+}$ hydroxocomplex, also known as titanyl cation $[TiO]^{2+}$ (dehydrated form). There are also coexisting $[Ti(OH)]^{3+}$ and $[Ti(OH)_3]^+$ [27]. For $Ni^{2+}$, hydrolysis starts at pH 6–7 and results in $[Ni(OH)]^+$ formation [28]. The initial experimentations were carried out using different aqueous neutral electrolytes successfully utilized in past research work, i.e., NaBr, NaCl, and $NaNO_3$ electrolytes. As the aqueous-based neutral electrolytes are safer, non-corrosive nature, non-flammable, and electrochemical stability as compared to toxic and highly flammable acidic electrolyte, these electrolytes have been selected. First, NaBr electrolyte has been used for machining of nitinol as it has proven suitability for titanium alloys, but till date, no experimentations are carried out for understanding the dissolution behavior of nitinol in wire electrochemical machining using tungsten wire electrode. From Fig. 3a–c, it is observed that a huge amount of sticky sludge is accumulated on the surface of nitinol for all the mentioned electrolyte concentrations due

to which machining has not been carried out uniformly and also produced uneven rough surface in the machined area. The oxidation state of Ni is same when oxides form from bromide without any electron transfer. The formation of $NiO_2$ is hardly possible which has the highest oxide, which basically can be formed at very high anodic potential (standard potential > 1.6 V SHE) hardly take place in bromide medium because the process of $Br^-$ oxidation to $Br_2$ is thermodynamically possible at much lower potential (standard potential ~ 1.1 V SHE), and electrode potential at constant voltage or current will not further increase before all $Br^-$ is transformed to $Br_2$. Bromide complexes of both Ni(II) and Ti(IV) are very weak, i.e., bromide competes with water bonding in coordination spheres of these ions; e.g., TiBr4 is known as a solid but undergoes immediate hydrolysis in water like $[NiBr_x]^{(2-x)+}$ or $[NiBr_x(H_2O)_{4-x}]^{(2-x)+}$. The highest capacity of $Br^-$ ions to permeate $TiO_2$ results in local dissolution, often known as pitting. $TiBr_4$ molecule clusters act as
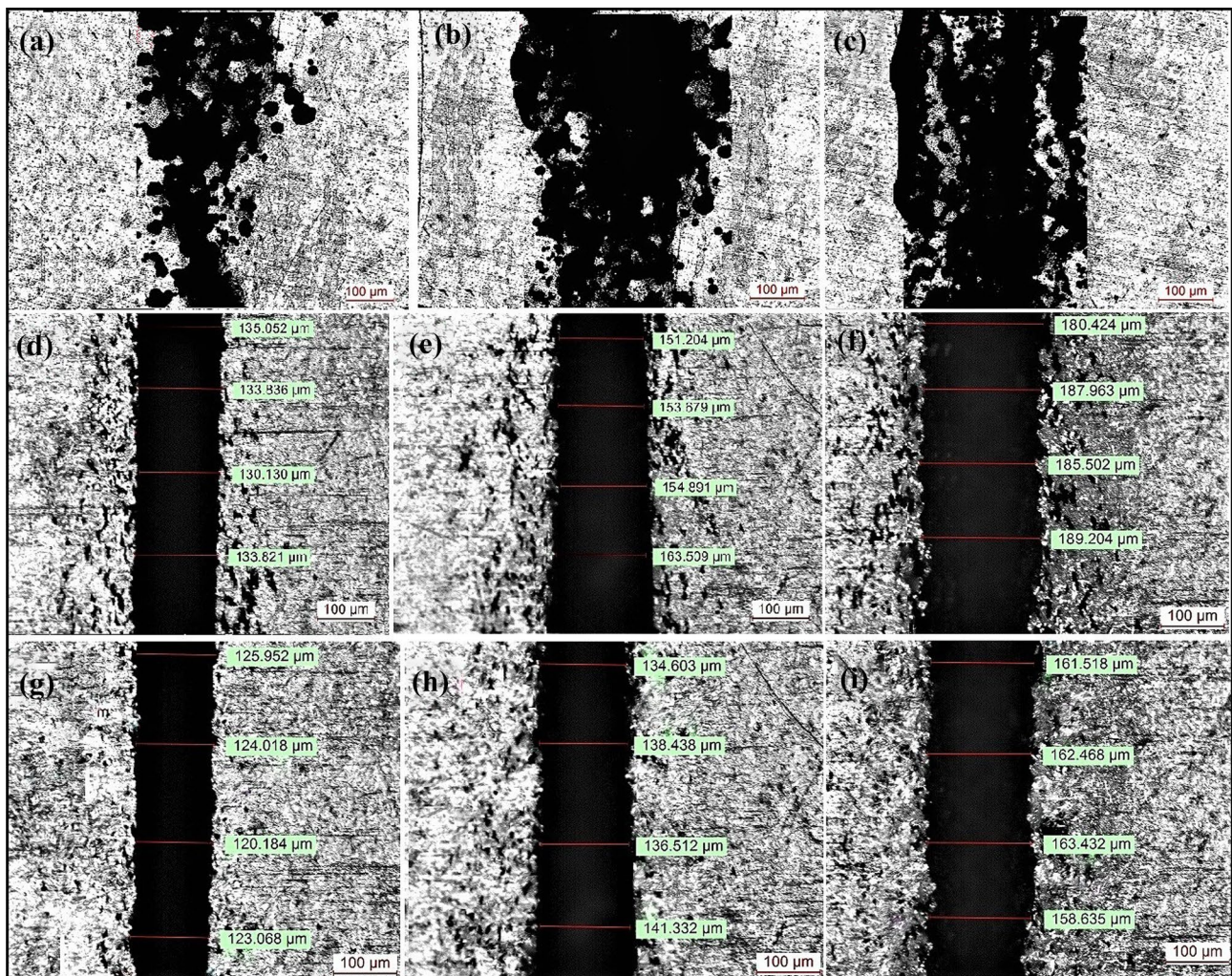


**Fig. 3** Fabricated microgrooves in NaBr (**a–c**), NaCl (**d–f**), and $NaNO_3$ (**g–i**) electrolytes at 0.2 M, 0.3 M, and 0.4 M concentration

the pit's nucleus, and they form in locations where the oxide layer electrical conductivity is higher. When the concentration of electrolyte is high, the anodic product TiBr$_4$ concentration at the nitinol surface is very high and would surpass the solubility product, precipitating the salt as a thick layer on the surface that would then obstruct the dissolving and produces hindrance in the machining of nitinol [27]. Further, it is seen from the Fig. 4a–c that the microgrooves' mean depth of 20.02 μm, 8.62 μm, and 10.86 μm has been obtained at 0.2 M, 0.3 M, and 0.4 M aqueous solution of NaBr electrolyte with increasing surface roughness Ra of 0.5777 μm, 0.8123 μm, and 0.9489 μm. It is observed that the aqueous

solution of NaBr electrolyte is not suitable for machining of nitinol during WECM.

Further experiments were carried out using aqueous electrolyte of NaCl. It can be seen from Figs. 3d–f and 4d–f that in the case of aqueous NaCl solution at 0.2 M electrolyte concentration, microgroove is fabricated with average groove width of 133.20 μm having a width overcut of 41.6 μm and a mean groove depth of 168.7 μm with a surface roughness Ra of 0.3994 μm. However, in the case of 0.3 M and 0.4 M electrolyte concentration, the anodic dissolution of nitinol is increased to a large extent with an increase in width overcut, i.e., 56.75 μm, and 69.6 μm and
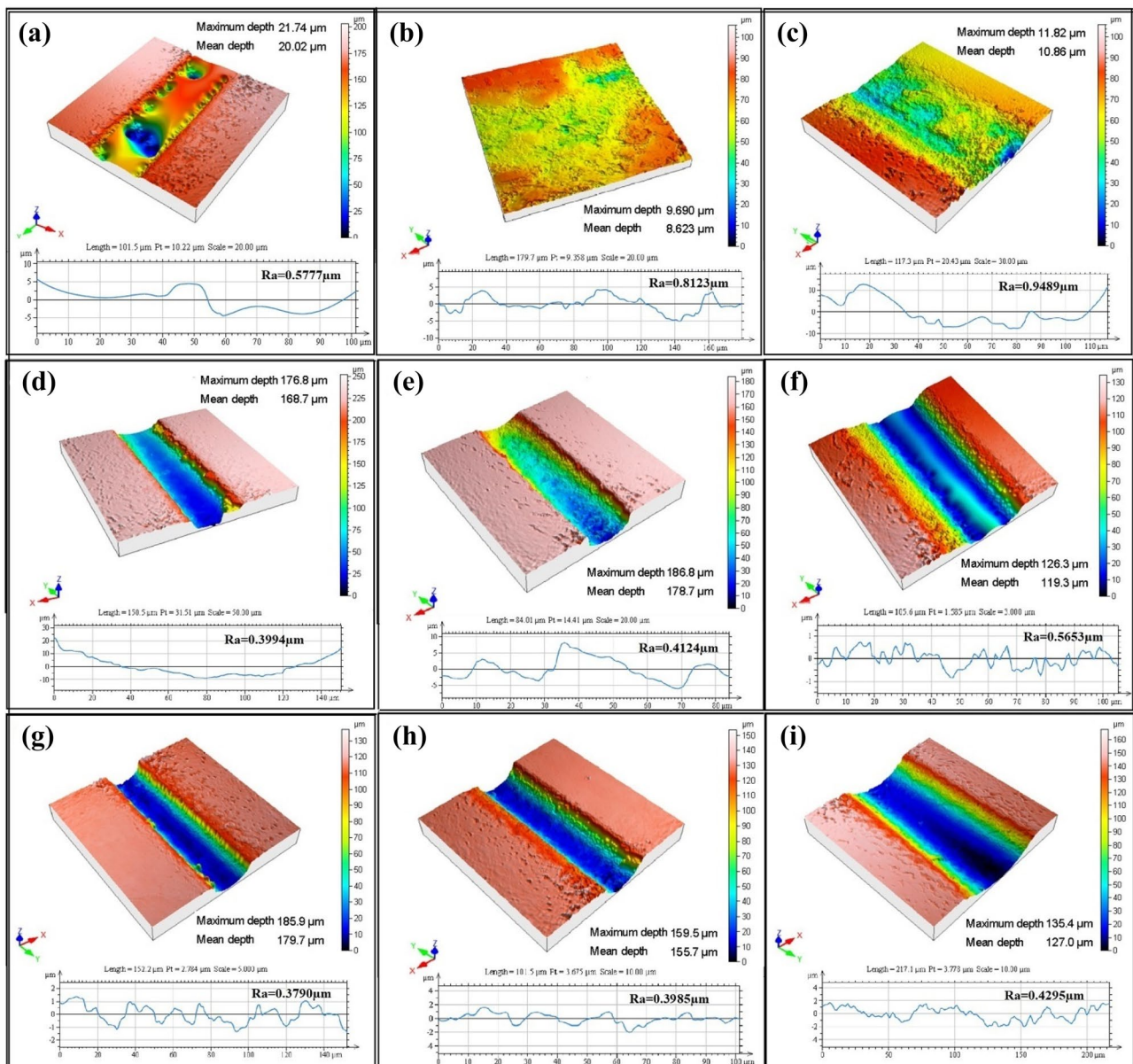


**Fig. 4** 3D profile with surface roughness and depth of microgrooves in NaBr (**a–c**), NaCl (**d–f**), and NaNO$_3$ (**g–i**) electrolytes at 0.2 M, 0.3 M, and 0.4 M concentration

surface roughness (Ra), i.e., 0.4124 μm and 0.5653 μm, respectively. It shows highly non-uniform dissolutions with non-uniformity in machined surface.

With chloride, complexes of both Ni(II) and Ti(IV) are also very weak, and only mixed aquachloride or hydroxochloride complexes are realistic; $TiCl_4$ tends to very fast hydrolysis and cannot survive, when solid oxochloride $Ti(OH)_nCl_{4-n}$ is more stable. $NiCl_2$ complex cannot be formed; $NiCl^+$ can dominate in background chloride solution but still coexists with Ni(II); $NiCl^+$ is a brief formula for aquachloride complex $[NiCl(H_2O)_3]^+$; hydrolysis with formation of $Ni(OH)^+$ starts at pH6 in this case, so at higher pH, mixed hydroxochloride complexes can be probably expected, but this issue is less studied. For Ti(IV) species in solution, no any chloride or aquachloride complexes can be formed, but hydroxooxochloride complexes are possible. To say, $[Ti(OH)_2Cl_4]^{2-}$ was reported in presence of background chloride, but of course, the number of bonded chlorides is much lower under conditions of presented experiments, so more or less general formula is $[Ti(OH)_x(H_2O)_y(Cl)_{4-x-y}]^{(4-y)+}$ [27].

It shows strong corrosion properties after hydrolysis affecting the surface during machining and required proper flushing for excellent corrosion resistance and better machinability. Another factor that strongly binds the nitinol surface is the production of $TiO_2$ once more on the anode. $NaNO_3$ is a well-known passivating electrolyte that is utilized in ECM-based micromachining to improve accuracy. Figures 3g–i and 4g–i in the case of neutral electrolyte aqueous $NaNO_3$ show that at lower concentrations of electrolyte, the sludge quantity adhering to the surface is smaller than at larger concentrations of electrolyte. Also, it has been observed that the accuracy parameters like groove width and mean groove depth increase with the increase in the electrolyte concentration as the dissolution rate increases; hence, the overcut increases. The average groove width of 123.30 μm, 137.72 μm, and 161.51 μm; mean groove

depth of 179.7 μm, 155.7 μm, and 127 μm; and the surface roughness (Ra) of 0.379 μm, 0.3985 μm, and 0.4295 μm are measured for 0.2 M, 0.3 M, and 0.4 M $NaNO_3$ electrolyte concentration, respectively; thus, a uniform dissolution of nitinol can be considered and smoother surface in comparison to NaCl electrolyte has been obtained.

The aforementioned dissolving process improves both the localized dissolution and the uniform electrochemical response in all electrolyte concentration conditions as compared to NaCl electrolyte solution. Figure 5a–c shows that the average groove width, mean groove depth, and the average surface roughness for all these electrolytes at different concentrations.

In the case of NaBr, machining of microgroove fabrication was not successful due to non-uniform dissolution, depth of machining is also very shallow throughout the nitinol surface area, the surface roughness (Ra) is also very high compared to both NaCl and $NaNO_3$ electrolytes, and the uniform dissolution was obtained in $NaNO_3$ electrolyte with smaller groove width, larger groove depth, and minimum average surface roughness (Ra). The energy-dispersive spectroscopy (EDS) analysis for FESEM image of nitinol surface in aqueous neutral solutions of NaCl, $NaNO_3$, and NaBr electrolytes under non-ozonated conditions that is shown in Fig. 6 reveals major components in the WECM machined surface layer such as Ti, Ni, C, and O. The machining parameters completely determine the surface morphology of the WECM process for nitinol shape memory alloy. The anodic dissolution of nitinol in simple aqueous NaBr solution is completely unstable, and non-proper machining has been occurring. It may be due to the production of highly sticky sludge by bromide content in the solution. When using a simple aqueous NaCl solution, it is demonstrated in EDS that chlorides and oxides are present on the surface in significant amounts which creates hindrance to the nitinol anodic dissolution. However, the metal removal is higher in NaCl solution due to its non-passivating behavior.
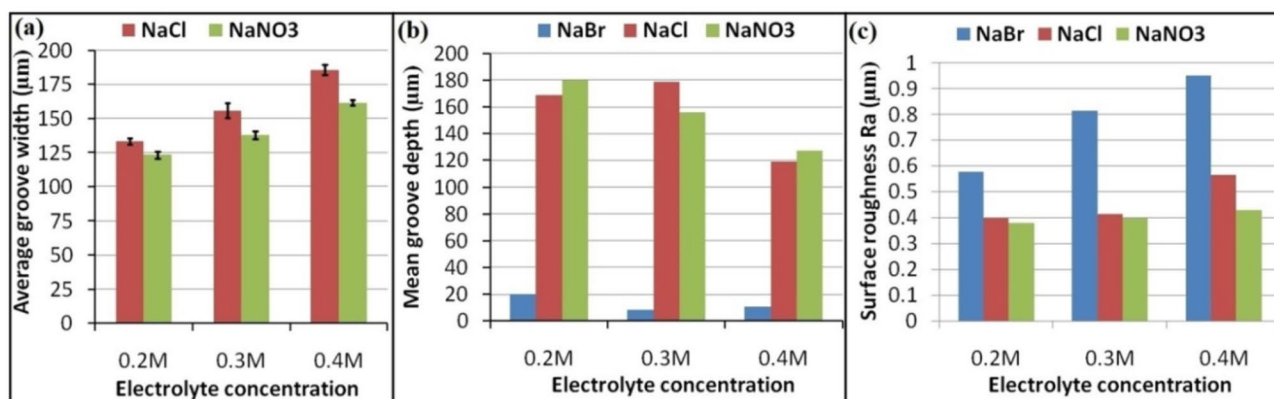


Fig. 5 Effect of different electrolyte concentrations on fabricated microgrooves for **a** average groove width, **b** mean groove depth, and **c** surface roughness (Ra)
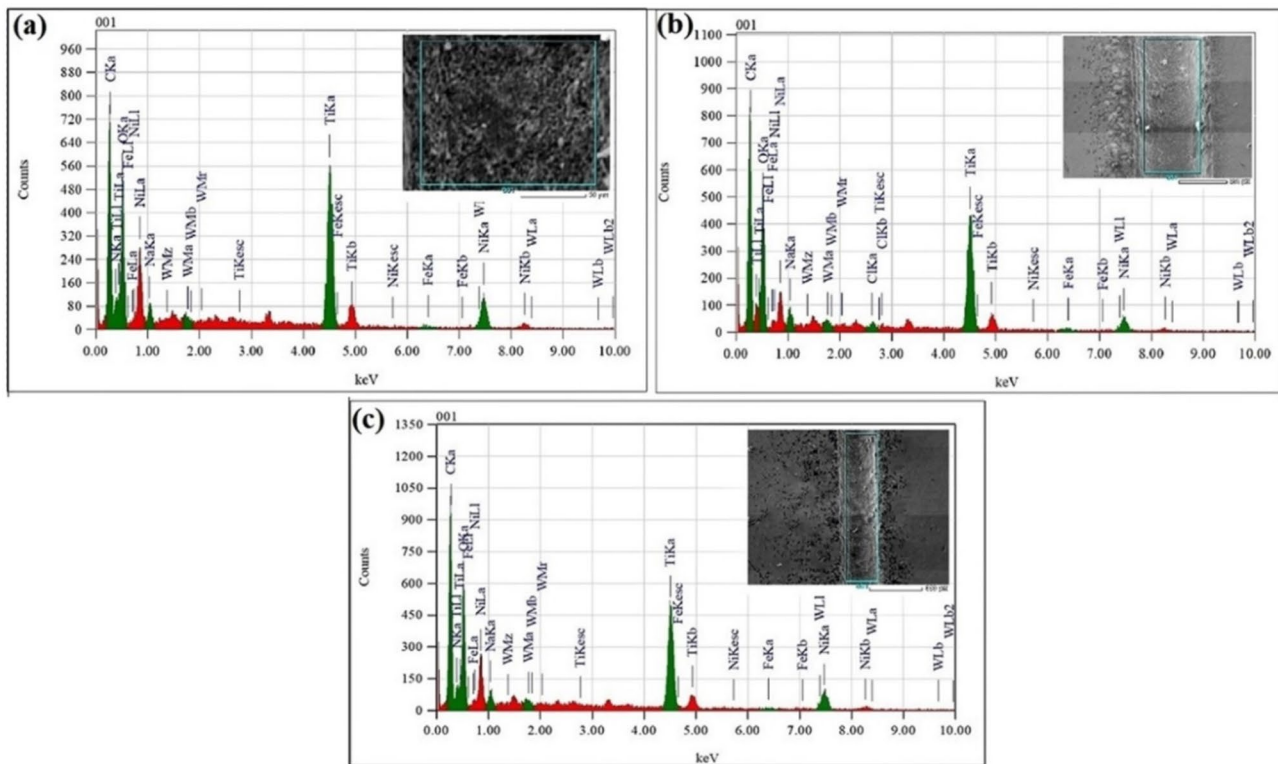
**Fig. 6** EDS of microgrooves surfaces with aqueous electrolytes **a** 0.2 M NaBr, **b** 0.2 M NaCl, and **c** 0.2 M NaNO$_3$

However, because of passivation in NaNO$_3$ due to its passivating behavior, the WECM process was characterized by oxide layers in aqueous NaNO$_3$ solution [6].

The machined surface is composed of a thin oxide layer of TiO$_2$, NiO, and consumed W electrode deposition particles, as well as the dissolved electrolyte medium which has been confirmed through XRD. The high activity of Ni and Ti atoms was attributed to TiO$_2$, TiC, and Ni complexes. WC occurs as a result of the deposition of the consumed W electrode. TiC and C are also the impacts of the all these electrolytes [7]. At low electrolyte concentration, the volume of Ti exceeds that of Ni. However, for the higher values of concentration, the quantity of Ni in the sludge is more than that of Ti. Table 2 shows the element composition of machined microgrooves surface, which demonstrates the existence of titanium, nickel, and oxygen at all electrolyte conditions in 0.2 M electrolyte concentration, showing the presence of titanium and nickel oxides. The oxygen and carbon contents in NaNO$_3$ electrolyte are lower as compared to NaBr and NaCl electrolyte. The nitinol dissolution occurs in two stages. The first process is the adsorption of OH ions results in passivity, and the second is the adsorption of anions (Br, Cl, NO$_3$, etc.). The adsorption of anions on the oxide layer produces soluble salts through cations from the oxide, resulting in the formation of pits. Once formed, these pits maintain to start local dissolution via the autocatalytic

process. The oxygen and carbon mass% is lower in NaNO$_3$ electrolyte solution compared to NaBr, and NaCl shows its suitability for surface improvement during machining of nitinol using WECM. WC is the result of it. Any organic contamination tends to form hydrocarbon under the electron beam on the sample surface, the amount of which can increase with measurement.

## Effect of mixed electrolyte on the accuracy and surface finish

The mixed electrolyte provides combined advantageous effects of constituents' electrolytes. For micromachining purposes, mixing of passivating and non-passivating electrolytes has been proven better for different materials. However, effect of mixing these electrolytes during micromachining of nitinol shape memory alloy has to be investigated. From the above experimental investigations for microgroove dimensions and surface roughness, it is observed that the NaNO$_3$ electrolyte is most suitable electrolyte for obtaining better dimensional accuracy and surface finish and NaCl for better metal removal rate. Therefore, further investigation has been carried out using mixed 0.2 M NaCl and 0.2 M NaNO$_3$ electrolyte and also used 0.2 M EDTA (ethylenedinitrilotetraacetic acid disodium salt dehydrate) as a complexing agent for enhancing the performance of machining during

**Table 2** EDS analysis for element composition of NaBr, NaCl, and NaNO$_3$

| Element (K) | NaBr | | NaCl | | NaNO$_3$ | |
|---|---|---|---|---|---|---|
| | mass% | atom% | mass% | atom% | mass% | atom% |
| Ni | 9.78 | 2.51 | 10.78 | 3.51 | 15.60 | 5.30 |
| Ti | 25.13 | 9.42 | 26.13 | 10.42 | 27.19 | 12.85 |
| O | 30.30 | 36.46 | 28.60 | 34.16 | 24.30 | 29.72 |
| C | 33.42 | 50.98 | 31.42 | 49.98 | 27.13 | 45.94 |
| Fe | 0.53 | 0.18 | 0.83 | 0.28 | 0.38 | 0.13 |
| Na | 0.66 | 0.38 | 1.66 | 1.38 | 1.51 | 1.28 |
| N | - | - | - | - | 3.38 | 4.71 |
| Cl | - | - | 0.49 | 0.26 | - | - |
| Br | 0.09 | 0.06 | - | - | - | - |
| W | - | - | - | - | 0.51 | 0.05 |

WECM. Primarily to understand the effect of mixed electrolyte on nitinol for understanding the dissolution mechanism in both the electrolytic conditions, the electrochemical impedance spectroscopy (EIS) has been conducted for mixed 0.2 M NaCl+0.2 M NaNO$_3$ and 0.2 M NaCl+0.2 M NaNO$_3$+0.2 M EDTA electrolyte, and results are obtained from the generated data and graphs as shown in Fig. 7. In electrochemical impedance spectroscopy (EIS), the working electrode is mounted on the cell stage and under the cell body. The counter and reference electrodes are held in place by the rubber stopper, which caps the cell body.

The imaginary impedance component (Z″) is shown against the real impedance component (Z′) for each excitation frequency in an EIS data shows Nyquist plot. The frequency (Hz) with respect to real component Z (Ω) and phase (°) enables the analysis of absolute impedance has been shown as Bode plot. To correct the capacitor's nonideal behavior, the constant phase element (CPE) concept can be applied to the modeling of an electrical double layer, and the surface-deposited double layer capacitor is linked in parallel with the polarization resistor (Rp), which is coupled

in series with the bulk resistor (Rs). The diameter of the semicircle also represents the polarization resistance. The Rs, Rp, and CPE components of the equivalent circuit are fitted to the semicircle, which depicts the quick oxidation and reduction kinetics. Nitinol alloys with high Rp have good corrosion resistance. Roughness values are low during an electrochemical reaction when there is decrease in corrosion rate. The polarization resistances (Rp) were measured and evaluated using the Nyquist and Bode plots. To support this result and quantify the corrosion behavior of the nitinol samples in both electrolytes, the EC system was modeled using equivalent electric circuits. Using the Nyquist and Bode plots of each circuit, the optimal circuit for each sample was determined. To account for electrolyte behavior and oxide layer resistance, each circuit has CPE and Rs, which causes a potential drop between the working electrode, nitinol, and the reference electrode, Ag/AgCl cell, generating errors, and Rp, which behaves like a resistor. In 0.2 M NaNO$_3$+0.2 M NaCl electrolyte as shown in Fig. 7a, the polarization resistance of the nitinol sample was 136 Ω shows higher corrosion resistance, while in 0.2 M
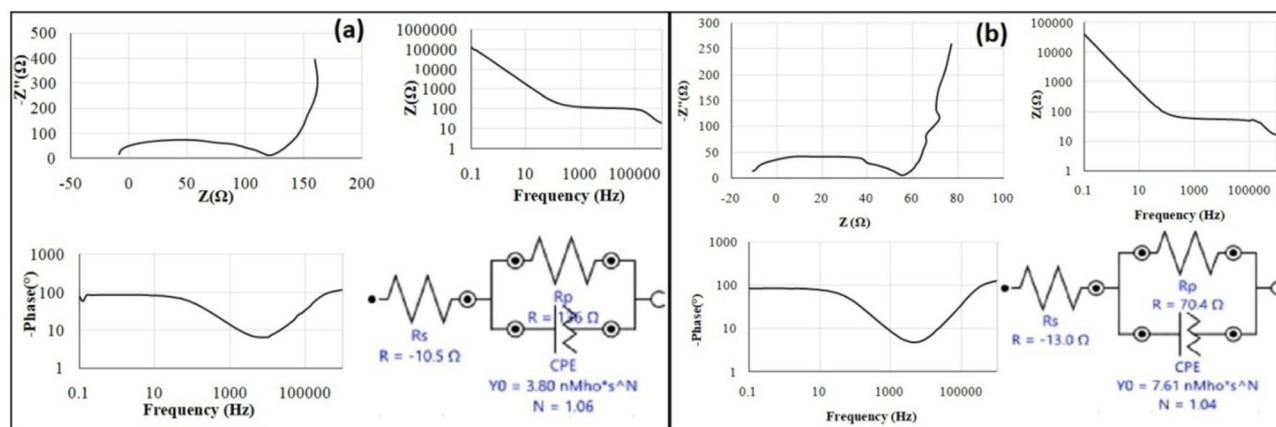


**Fig. 7** EIS with mixed electrolytes **a** 0.2 M NaCl+0.2 M NaNO$_3$ and **b** 0.2 M NaCl+0.2 M NaNO$_3$+0.2 M EDTA

NaCl + 0.2 M NaNO$_3$ + 0.2 M EDTA electrolyte, it was 70.4 Ω shown in Fig. 7b shows lower corrosion resistance as indicated by the values of the resistances Rp and Rs. The lower current density produces due to lower Rp in 0.2 M NaCl + 0.2 M NaNO$_3$ + 0.2 M EDTA electrolyte leading to formation of smooth surface and enhancement in surface finish as compared to 0.2 M NaNO$_3$ + 0.2 M NaCl electrolyte. The EIS data support the notion that the corrosion resistance of nitinol alloy is linked to the formation of a strong titanium oxide layer on the surface. The current investigations show that process-induced surface smoothing and the spontaneous formation of a passive layer boost the corrosion resistance of nitinol.

The smoothening of the surface and the formation of a thin coating of TiO$_2$ on it are associated with the alloy's higher corrosion resistance and uniform corrosion behavior. It is widely acknowledged that the outcome of an EIS measurement can be utilized to effectively define the surface state of a material. The suitability of an acceptable electrolyte for further machining during WECM was determined using this electrochemical characterization investigation for nitinol utilizing 0.2 M NaCl + 0.2 M NaNO$_3$ and 0.2 M NaCl + 0.2 M NaNO$_3$ + 0.2 M EDTA electrolytes. The capacity to create smooth surfaces makes NaNO$_3$ solutions the preferred electrolyte. However, the passive layer that the NaNO$_3$ electrolyte forms on the surfaces further impedes accurate machining, leading to normal machining capabilities. A correct machining performance is required while fabricating nitinol microfeatures. So, in order to improve the performance of the WECM, NaCl is mixed into the aqueous NaNO$_3$ electrolyte. Among all these aqueous neutral electrolyte solutions used under mixed electrolyte conditions, both the electrolytes were capable to effectively machine nitinol with improved anodic dissolution efficiency. However, the oxide layer formed on the machine surface during machining with 0.2 M NaCl + 0.2 M NaNO$_3$ electrolyte impairs the machining accuracy and surface finish which also affects the machined surface due formation of pitting near the sidewall of the microgroove as shown in Fig. 8. It is observed that the average groove width of 118.35 μm with a mean depth of 188.7 μm and average surface roughness Ra of 0.3333 μm have been obtained in mixed 0.2 M NaCl + 0.2 M NaNO$_3$ electrolyte. Also, tapering effect has been found on the top initial machined surface of the nitinol compared to bottom surface, and homogeneity of sidewall of the microgroove is poor in mixed 0.2 M NaCl + 0.2 M NaNO$_3$ electrolyte.

The addition of EDTA as a complexing agent helps to reduce excessive oxide layer on the surface of nitinol due to lower passivating effect, and hence, clean surface will be existing for machining during WECM. With the chemical formula C$_{10}$H$_{14}$N$_2$Na$_2$O$_8$.2H$_2$O, i.e., ethylenedinitrilotetraacetic acid disodium salt, Na$_2$H$_2$EDTA, i.e., Na$_2$H$_2$Y where Y is C$_{10}$H$_{12}$O$_2$, EDTA disodium salt is a kind of complexing agent that
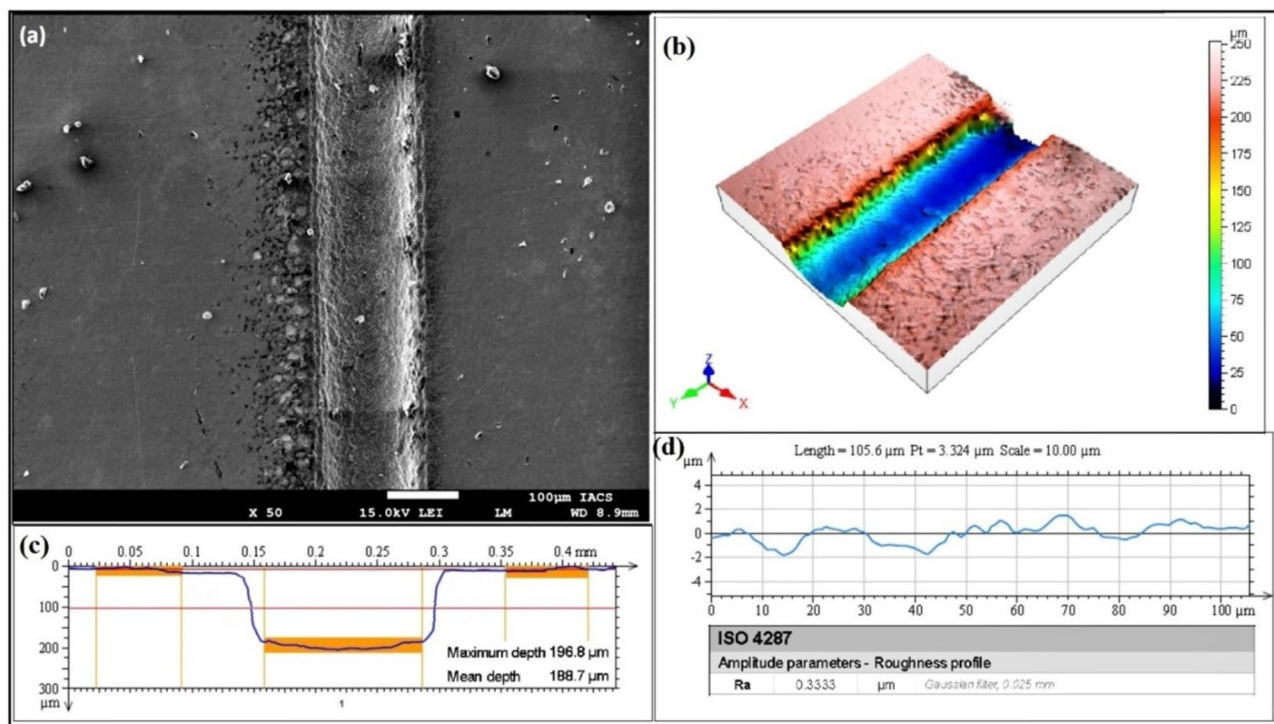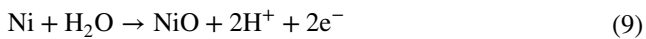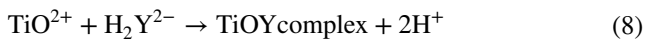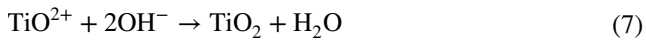


**Fig. 8** **a** FESEM, **b** 3D surface, **c** mean depth, and **d** roughness profile of fabricated microgroove using mixed 0.2 M NaNO$_3$ + 0.2 M NaCl electrolyte

has the capacity to interact with most metal ions and produce a soluble complex molecule. The probable chemical reactions in EDTA for nitinol are as follows [20, 29]:

At cathode:

$$2H^+ + 2e^- \rightarrow H_2 \uparrow \tag{5}$$

At the interface of anode and electrolyte:

$$2H_2O \rightarrow 4H^+ + O_2 \uparrow + 4e^- \tag{6}$$

$$TiO^{2+} + 2OH^- \rightarrow TiO_2 + H_2O \tag{7}$$

$$TiO^{2+} + H_2Y^{2-} \rightarrow TiOYcomplex + 2H^+ \tag{8}$$

$$Ni + H_2O \rightarrow NiO + 2H^+ + 2e^- \tag{9}$$

$$NiO + 2H^+EDTA \rightarrow Ni^{2+}EDTA + H_2O \tag{10}$$

It is discovered that increasing the $TiO_2$ layer reduces the metal removal at higher electrolyte concentrations. Because $NaNO_3$ is passive in nature, it promotes the formation of a passive layer on the surface of nitinol, slowing the dissolution process and reducing overcut, and NaCl is non-passive in nature that improves the material removal rate. If parallel

oxygen evolution takes place on anode, pH near the surface is decreasing. However, if the wire cathode is close to anode, the pH value near anode can be affected by pH increase near cathode (which results from hydrogen evolution). Because EDTA is a chelating agent that forms soluble complexes with titanium ions, it can be used to minimize the production of $TiO_2$ layers in these electrolytes. Hence, the combination of these electrolytes improved the performance of machining in terms of accuracy, material removal rate, and surface finish as shown in Fig. 9.

The pitting effect has been lowered, and the homogeneity of microgroove has improved the addition of EDTA as compared to the microgroove fabricated with mixed 0.2 M $NaNO_3$ + 0.2 M NaCl electrolyte shown in Fig. 8. It has been observed that the mean depth of machined microgroove with mixed 0.2 M NaCl + 0.2 M $NaNO_3$ + 0.2 M EDTA electrolyte has been improved to 232.9 μm which is more as compared to mean depth of mixed NaCl + $NaNO_3$ electrolyte, but tapering effect also increased. As far as width overcut is concerned in both these combination of electrolyte, there is no remarkable difference. Also, the average surface roughness (Ra) is 0.2790 μm in this electrolyte which is better than mixed NaCl + $NaNO_3$ shows improvement in the machining process. Further, the analysis for machined surfaces has
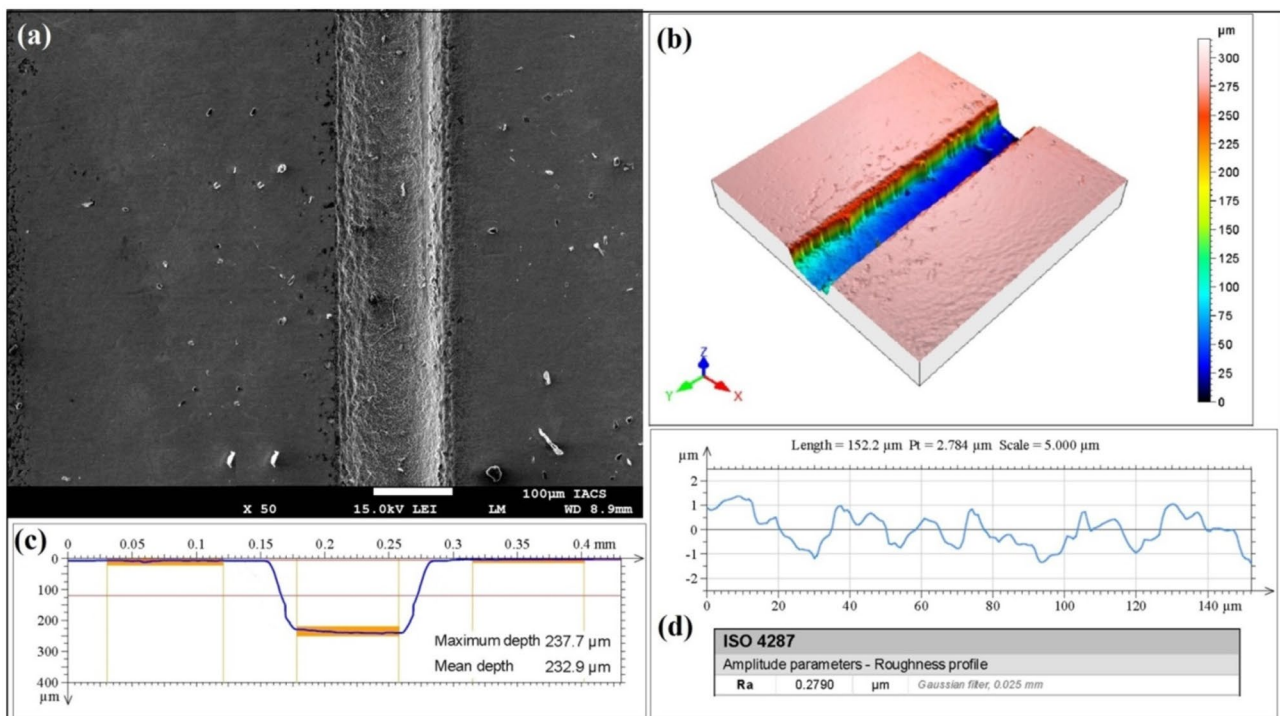


**Fig. 9** **a** FESEM, **b** 3D surface, **c** mean depth, and **d** roughness profile of fabricated microgroove using mixed 0.2 M NaCl + 0.2 M $NaNO_3$ + 0.2 M EDTA electrolyte

been carried out using mixed 0.2 M NaCl + 0.2 M NaNO$_3$ and 0.2 M NaCl + 0.2 M NaNO$_3$ + 0.2 M EDTA aqueous electrolyte solutions using EDS and FESEM images with generated plots are shown in Fig. 10. The oxygen concentration is 20% without EDTA and 17.99% with EDTA, according to the EDS results presented in Table 3.

It has been confirmed from the EDS analysis that the lower content of oxygen in presence of EDTA forms thin oxide layer on the machining surface and occurs uniform dissolution during machining. This implies that an EDTA-based solution forms only a thin coating of titanium oxide, allowing for the machining of microgrooves with fewer overcuts and more mean depth. As seen in EDS, solutions containing EDTA create less current density than solutions containing no EDTA. The mixed electrolyte with addition of EDTA has better machining capability due to uniform dissolution compared to machining in individual electrolytes producing larger oxygen and carbon contents. However, NaCl electrolyte produces large current. When 0.2 M EDTA is present in the mixed 0.2 M NaCl + 0.2 M NaNO$_3$ electrolyte solution, this results in a uniform and controlled anodic dissolution of nitinol, which is also responsible for the reduction in overcut and increase in mean depth with better surface finish as compared to mixed 0.2 M NaCl + 0.2 M NaNO$_3$ electrolyte solution without EDTA.

## Effect of ozonated mixed electrolytes on the accuracy and surface finish

The assertion of the experimental findings that the ozonated electrolytes and its combination typically offer superior outcomes in case of nitinol shape memory alloy dissolving during WECM deserves more investigation. The ozone can mix with the electrolyte in machining chamber and evaporate immediately after cleaning sludge and dissolved products which renew the electrolyte for further machining.

**Table 3** EDS analysis for element composition of mixed electrolyte

| Element (K) | NaCl + NaNO$_3$ | | NaCl + NaNO$_3$ + EDTA | |
|---|---|---|---|---|
| | mass% | atom% | mass% | atom% |
| Ni | 21.87 | 9.23 | 23.16 | 9.04 |
| Ti | 30.16 | 12.57 | 32.33 | 18.04 |
| O | 20.00 | 27.39 | 17.99 | 26.08 |
| C | 23.19 | 45.20 | 20.78 | 39.67 |
| Fe | 0.36 | 0.14 | 0.44 | 0.18 |
| Na | 1.66 | 1.54 | 0.88 | 0.88 |
| N | 2.35 | 3.58 | 3.68 | 6.02 |
| Cl | 0.41 | 0.24 | - | - |
| W | - | - | 0.74 | 0.09 |

From the above investigation, it is observed that the mixed electrolytes have capability to create smooth surfaces with fewer overcuts in width and more mean depth in fabricated microgrooves. However, the passive layer that the NaNO$_3$ electrolyte forms on the surfaces and large amount of sludge produced on the machining surface in NaCl electrolyte due to more metal removal further impedes accurate machining, leading to low grade machining capabilities. A correct machining performance is required while fabricating nitinol microfeatures. So, in order to improve the performance of the WECM, ozone gas is pressurized into the mixed aqueous 0.2 M NaCl + 0.2 M NaNO$_3$ by creating an ozonated mixed aqueous 0.2 M NaCl + 0.2 M NaNO$_3$ electrolyte. With the ozonated aqueous solution, metal removal is shown to be greater than with the non-ozonated electrolyte for all runs. This results in the prevention of an ozonation-caused passive layer and removal of sludge. Ozone (O$_3$) is enhanced to increase the oxidizing ability and corrosive behavior of basic aqueous electrolytes. Ozone must be created in an area where it will be consumed since it is extremely unstable and quickly becomes O$_2$. This explains how adding ozonated aqueous NaCl and NaNO$_3$ solution to the WECM for nitinol
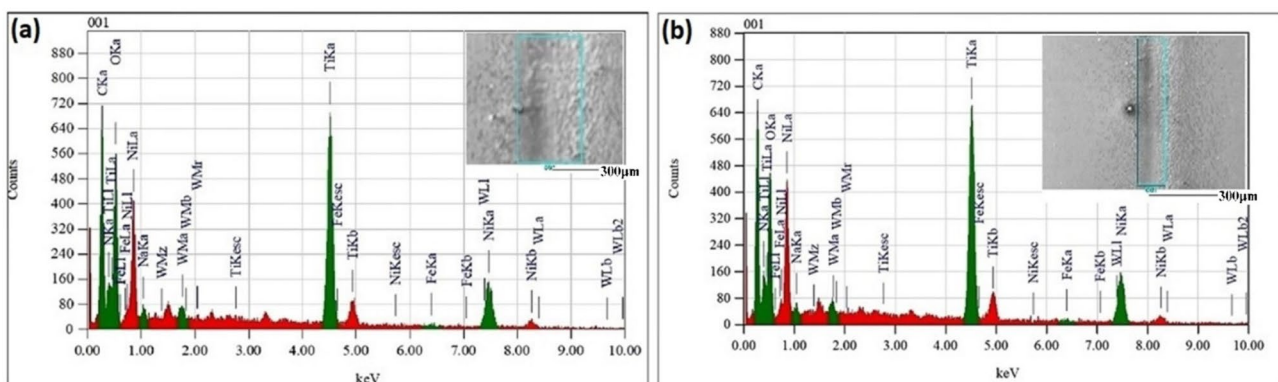


**Fig. 10** EDS of microgrooves surfaces with mixed aqueous electrolytes **a** 0.2 M NaCl + 0.2 M NaNO$_3$ and **b** 0.2 M NaCl + 0.2 M NaNO$_3$ + 0.2 M EDTA

affects how well the machine can function. Ozone is a powerful oxidant with a relatively short half-life that has been employed in many different chemical applications.

The oxidative capability of ozone is increased via controlled ozone breakdown. The flow rate of the electrolyte is taken into account since it is required to assist ozonation for stability and to remove oxides and sludge from the tiny gap. The surface of the workpiece would react with hydroxyl ions to produce hydroxides, which would then precipitate as sludge. For all experiments, it has been found that metal removal is greater for the ozonated aqueous solution. This is as a result of the $O_3$ mixed electrolyte's efficient removal of deposited contaminants from the surface. Deposits are continually removed, leaving a clean surface that may be machined further. The ozonation technique fully eliminates the metal sludge that is accumulated on the workpiece surface. Oxides on the workpiece surface can be removed with the help of the ozone, which frequently breaks down into oxygen form. Surface roughness is caused by active dissolving on the workpiece surface, which is caused by the present electrolyte concentration settings and ozonation during machining of nitinol.

Figure 11 shows the FESEM, mean depth, 3D surface, and roughness profile of machined microgroove at 0.2 M mixed ozonated aqueous $NaCl + NaNO_3$ electrolyte. Ozone presence has a greater impact on the specimen's surface. The anodic dissolution is impacted by the increase in electrolyte

conductivity. By rapidly oxidizing an oxide layer on the metal surface, ozonation exposes the workpiece's brand-new surface. As a consequence, ozonation effectively removes sludge and oxides, leaving the surface clean and improving surface roughness Ra. There are no more deposits on the uniformly machined surface. The removal of oxides from the nitinol sample surface increases the metal removal in the ozonated aqueous 0.2 M NaCl + 0.2 M $NaNO_3$ electrolyte. Ozone breaks down into extremely reactive secondary oxidants made of hydroxyl and peroxyl radicals, which react quickly with dissolved oxide and metal hydroxide complexes. The nitrate is converted into nitrite during the anodic metal dissolution of ECM method using aqueous $NaNO_3$ as an electrolyte. The primary cause of the passive layer development on the workpiece surface is nitrite content. This passive layer acts as an insulating layer and is difficult to remove, slowing the anodic dissolution rate. Further, The NaCl electrolyte has a tendency to remove material to a larger extent due to which more sludge generated on the workpiece surface. The buildup of sludge and oxides prevents the workpiece from having a superior surface finish. However, the availability of oxygen owing to the constant flow of ozone cleans the surface and eliminates the contaminants. The radicals created by ozonation lead to hydrogen peroxide, which enhances the efficiency of machining. From the experimental investigation, the microgroove average width of 115.365 μm, mean depth of



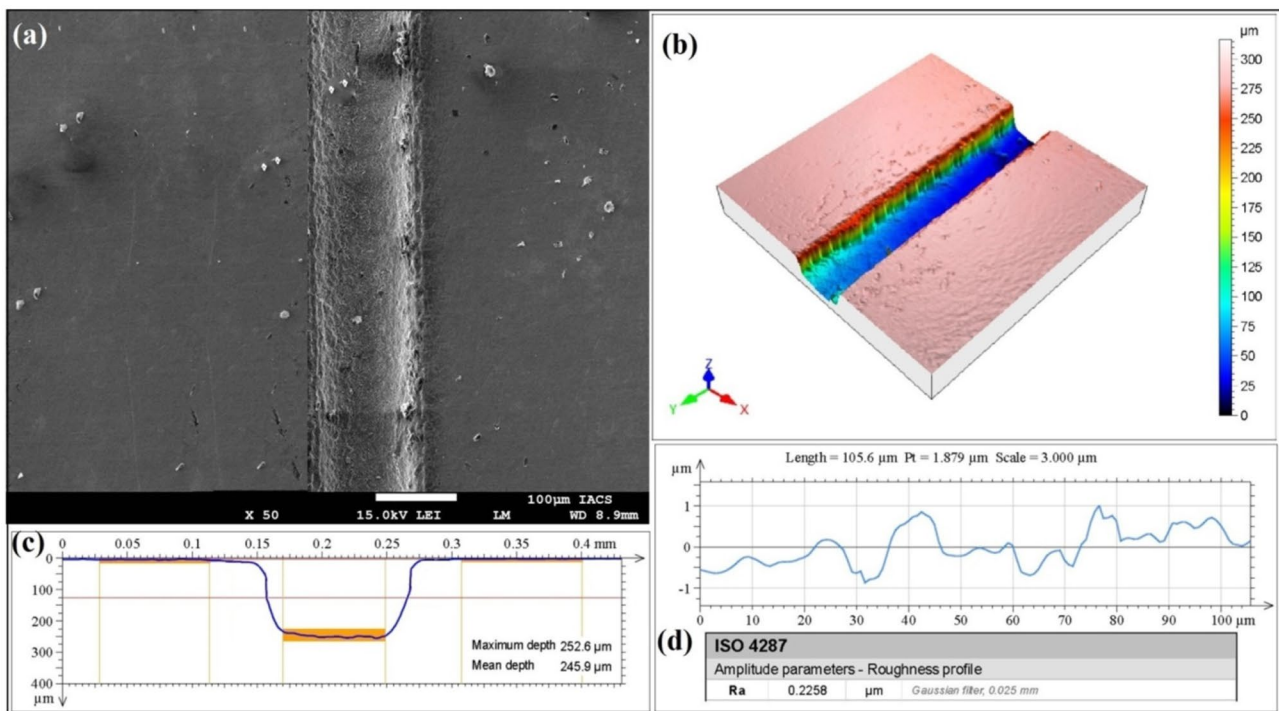**Fig. 11** **a** FESEM, **b** 3D surface, **c** mean depth, and **d** roughness profile of fabricated microgroove using mixed ozonated 0.2 M NaCl + 0.2 M $NaNO_3$ electrolyte

245.9 μm, and average surface roughness (Ra) of 0.2258 μm have been obtained which shows improved results as compared to mixed aqueous 0.2 M NaCl + 0.2 M NaNO₃ due to application of ozonization. The pitting effect is very less, and homogeneity has been improved in this electrolyte as compared to non-ozonated mixed NaCl + NaNO₃ electrolyte.

As it is seen in the investigation of mixed 0.2 M NaCl + 0.2 M NaNO₃ + 0.2 M EDTA that the dimensional characteristics and surface finish have been improved compared to mixed 0.2 M NaCl + 0.2 M NaNO₃ electrolyte, further analysis has been carried out with mixed ozonated 0.2 M NaCl + 0.2 M NaNO₃ + 0.2 M EDTA electrolyte solution. The FESEM image, mean depth, 3D surface, and roughness profile of machined microgroove with 0.2 M mixed ozonated aqueous 0.2 M NaCl + 0.2 M NaNO₃ + 0.2 M EDTA electrolyte are shown in Fig. 12. From the experimental investigation, the microgroove average width of 105.86 μm, mean depth of 264.6 μm, and average surface roughness (Ra) of 0.1346 μm have been obtained with mixed ozonated aqueous 0.2 M NaCl + 0.2 M NaNO₃ + 0.2 M EDTA electrolyte during nitinol machining. The homogeneous microgroove with smooth surface finish has been obtained, and pitting effect was not seen on the sidewall of the machined microgrooves with negligible tapering effect. It shows that mixed ozonated 0.2 M NaCl + 0.2 M NaNO₃ + 0.2 M EDTA electrolyte solution has been proven as the best electrolyte combination for obtaining better accuracy and surface finish during

microgroove machining of nitinol shape memory alloy using wire electrochemical machining. The EDS analysis for machined surfaces of ozonated mixed 0.2 M NaCl + 0.2 M NaNO₃ and 0.2 M NaCl + 0.2 M NaNO₃ + 0.2 M EDTA aqueous electrolyte solutions is shown in Fig. 13. The peaks of the titanium Ti and nickel Ni have been improved, while peaks of oxygen O and carbon C have been reduced. It shows that the use of ozonization in electrolyte has great influence on formation of oxide layer on the machining surface of the nitinol to produce uniform anodic dissolution.

The EDS findings reveal that oxygen present on the machined surface has lower value, implying that the nitinol surface has no more passivity in the electrolyte solution containing EDTA under ozonated condition compared with other non-ozonated conditions. In the case of the ozonated 0.2 M NaCl + 0.2 M NaNO₃ + 0.2 M EDTA electrolyte, this implies that the machined surface dissolves uniformly.

The oxygen concentration (mass%) is 18.44% without EDTA and 14.66% with EDTA in ozonated conditions of both these electrolytes, according to the EDS results presented in Table 4.

This implies that an EDTA-based solution forms only a very thin coating of titanium oxide as compared to non-ozonated mixed simple aqueous electrolytes, allowing for the machining of homogeneous microgrooves with more depth of penetration due to uniform anodic dissolution of nitinol during WECM. When comparing results for average
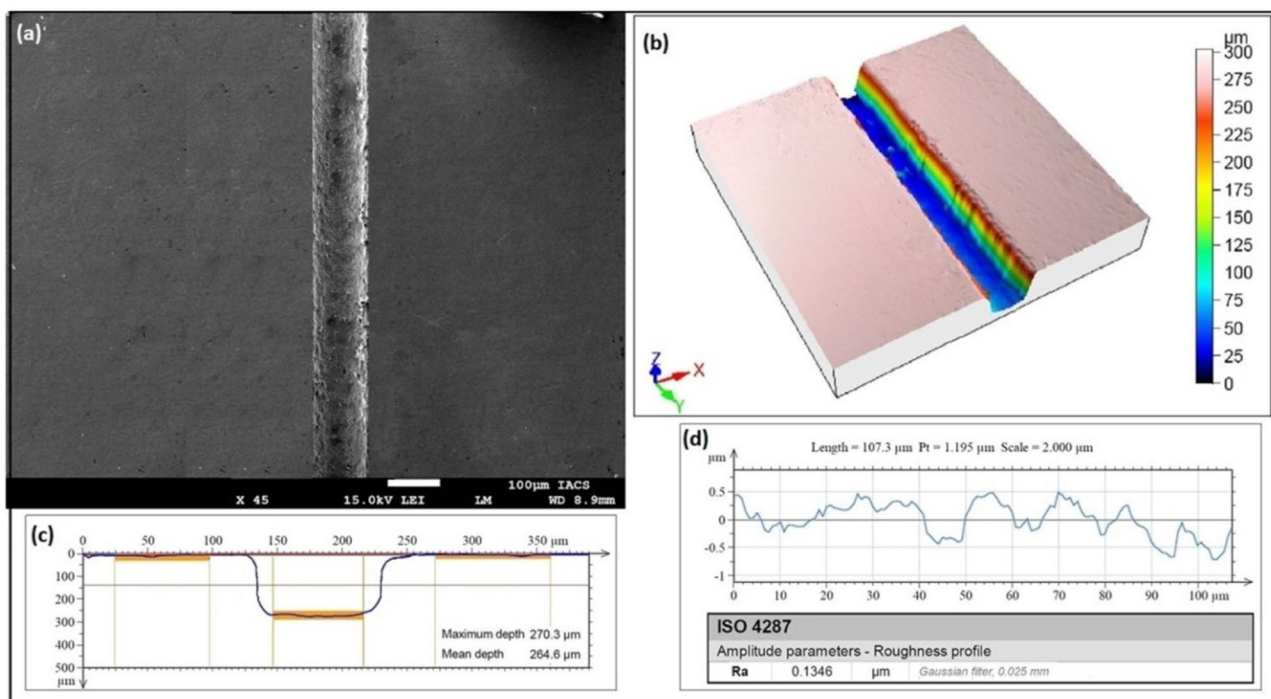


**Fig. 12** **a** FESEM, **b** 3D surface, **c** mean depth, and **d** roughness profile of fabricated microgroove using mixed ozonated 0.2 M NaCl + 0.2 M NaNO₃ + 0.2 M EDTA electrolyte
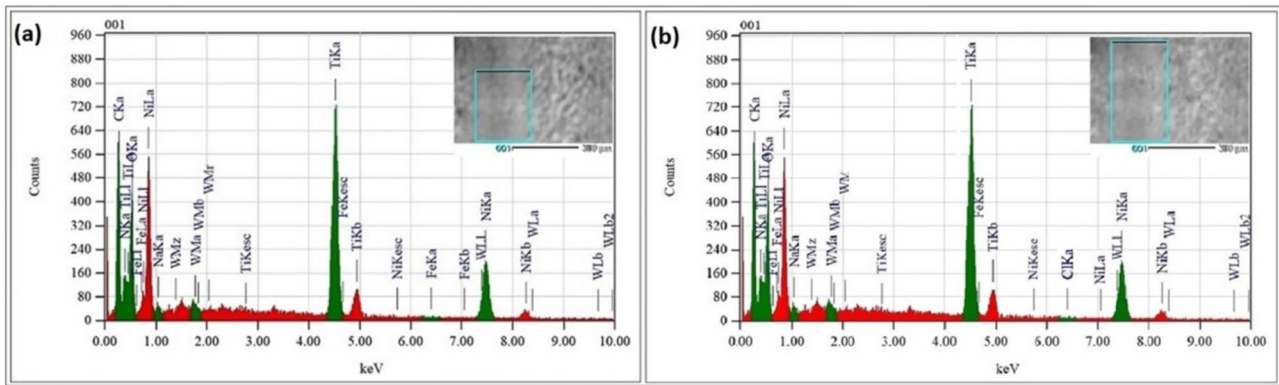
**Fig. 13** EDS of microgrooves surfaces with ozonated mixed aqueous electrolytes **a** 0.2 M NaCl+0.2 M NaNO$_3$ and **b** 0.2 M NaCl+0.2 M NaNO$_3$+0.2 M EDTA

groove width, mean depth, and surface roughness (Ra) for mixed 0.2 M NaCl+0.2 M NaNO$_3$ and mixed 0.2 M NaCl+0.2 M NaNO$_3$+0.2 M EDTA electrolytes under non-ozonated and ozonated conditions are depicted in Fig. 14, it is observed that that the average groove widths have no more differences in dimensional characteristics. However, there is improvement in mean depth and surface roughness Ra. The minimum mean depth has been obtained with mixed 0.2 M NaCl+0.2 M NaNO$_3$ under non-ozonated condition, and maximum mean depth has been obtained with mixed 0.2 M NaCl+0.2 M NaNO$_3$+0.2 M EDTA under ozonated condition. In the same way, surface roughness Ra is maximum with NaCl+NaNO$_3$ under non-ozonated condition and minimum with mixed 0.2 M NaCl+0.2 M NaNO$_3$+0.2 M EDTA under ozonated condition. The average groove width is 118.35 μm, 115.365 μm, 112.68 μm, and 105.86 μm; mean depth is 188.7 μm, 232.9 μm, 245.9 μm, and 264.6 μm; and the surface roughness (Ra) of the machined surface achieved was 0.3333 μm, 0.2790 μm, 0.2258 μm, and 0.1346 μm for mixed 0.2 M NaCl+0.2 M NaNO$_3$, mixed

0.2 M NaCl+0.2 M NaNO$_3$+0.2 M EDTA, ozonated mixed 0.2 M NaCl+0.2 M NaNO$_3$, and ozonated mixed 0.2 M NaCl+0.2 M NaNO$_3$+0.2 M EDTA electrolytes. It shows that ozonated mixed 0.2 M NaCl+0.2 M NaNO$_3$+0.2 M EDTA electrolyte has been proven as the most suitable electrolyte combination to achieve better dimensional characteristics and surface finish of nitinol during wire electrochemical machining.

## Fabrication of microslits with ozonated mixed electrolytes

The fabrication of perfect microslits is complicated for WECM due to the inaccuracies and the poor surface finish developed during machining. This investigation verified that the use of EDTA as a complexing agent, in combination with ozonated NaCl and NaNO$_3$ electrolyte, can improve the microfeatures accuracy of nitinol. The process used to fabricate the microslits involved wire electrochemical machining where constant wire feed has been given for material removal to fabricate a microslit on the nitinol sheet of 200-μm thickness. The concentration of the mixed 0.2 M NaCl+0.2 M NaNO$_3$ and mixed 0.2 M NaCl+0.2 M NaNO$_3$+0.2 M EDTA electrolyte was kept constant, while other machining parameters, like pulse duty ratio of 50%, pulse frequency of 250 kHz, initial IEG of 50 μm, wire diameter of 50 μm, and pulse voltage of 5 V at a wire feed rate of 1.4 μm/s, remained unchanged. The optical images are presented in Fig. 15. For ozonated mixed 0.2 M NaCl+0.2 M NaNO$_3$ electrolyte and mixed 0.2 M NaCl+0.2 M NaNO$_3$+0.2 M EDTA ozonated electrolyte, the average slit width is 123.34 μm and 106.40 μm, respectively, whereas the surface roughness (Ra) is calculated as 0.1546 μm and 0.1261 μm, respectively, for the corresponding electrolytes measured using coherent correlation interferometer (CCI).

**Table 4** EDS analysis for element composition ozonated mixed electrolytes

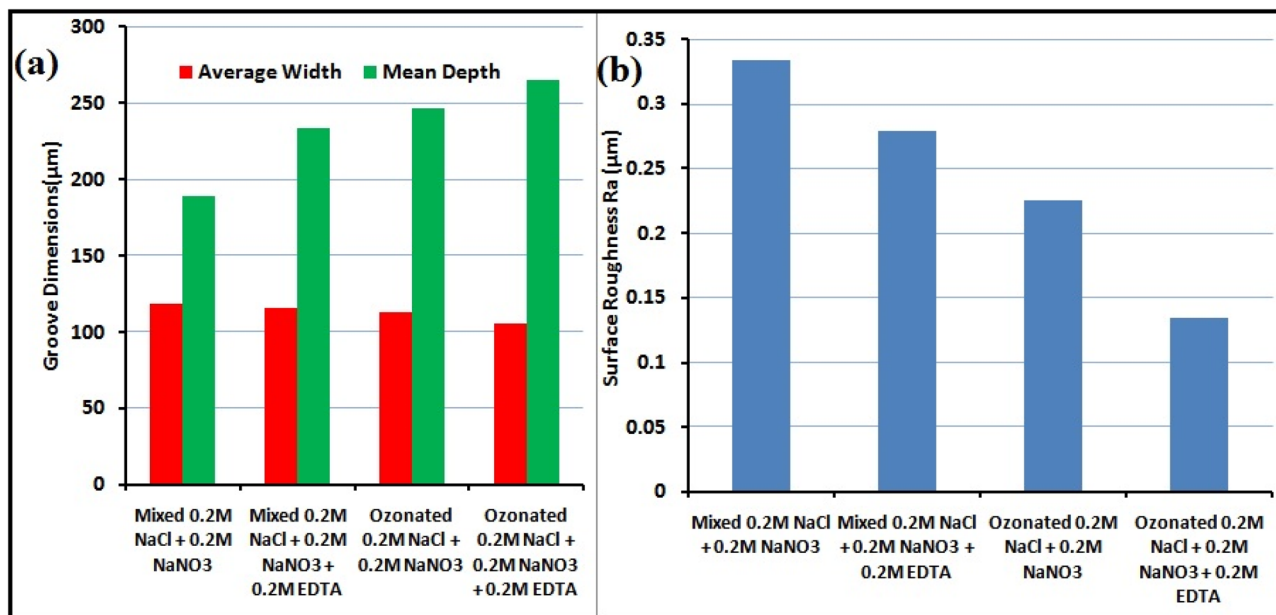| Element (K) | Ozonated NaCl+NaNO$_3$ | | Ozonated NaCl+NaNO$_3$+EDTA | |
|---|---|---|---|---|
| | mass% | atom% | mass% | atom% |
| Ni | 25.16 | 10.11 | 32.11 | 19.41 |
| Ti | 32.09 | 14.73 | 33.74 | 19.17 |
| O | 18.44 | 27.18 | 14.66 | 20.18 |
| C | 18.03 | 39.32 | 14.63 | 33.26 |
| Fe | 0.61 | 0.26 | - | - |
| Na | 0.85 | 0.87 | 0.62 | 0.69 |
| N | 4.34 | 7.30 | 3.92 | 7.08 |
| Cl | 0.24 | 0.20 | 0.24 | 0.20 |
| W | 0.24 | 0.03 | 0.08 | 0.01 |

**Fig. 14** Comparison of microgrooves in various mixed ozonated electrolytes for **a** average width and mean depth and **b** surface roughness Ra

Further, it can be seen that the slit width at start and end has negligible variations in measured dimensions with better uniformity. The inlet and outlet have consistent and uniform dissolution due to proper flushing and renewal of fresh electrolytes throughout the machining. Thus, with the usage of the EDTA as a complexing agent in combination with

$NaCl + NaNO_3$ electrolyte, accurate and precise microslits with lowest surface roughness could be successfully fabricated. The machined surface conditions using ozonated 0.2 M $NaCl + 0.2$ M $NaNO_3$ with the measured average surface roughness values (Ra) of 0.2345 μm and mixed ozonated 0.2 M $NaCl + 0.2$ M $NaNO_3 + 0.2$ M EDTA electrolyte
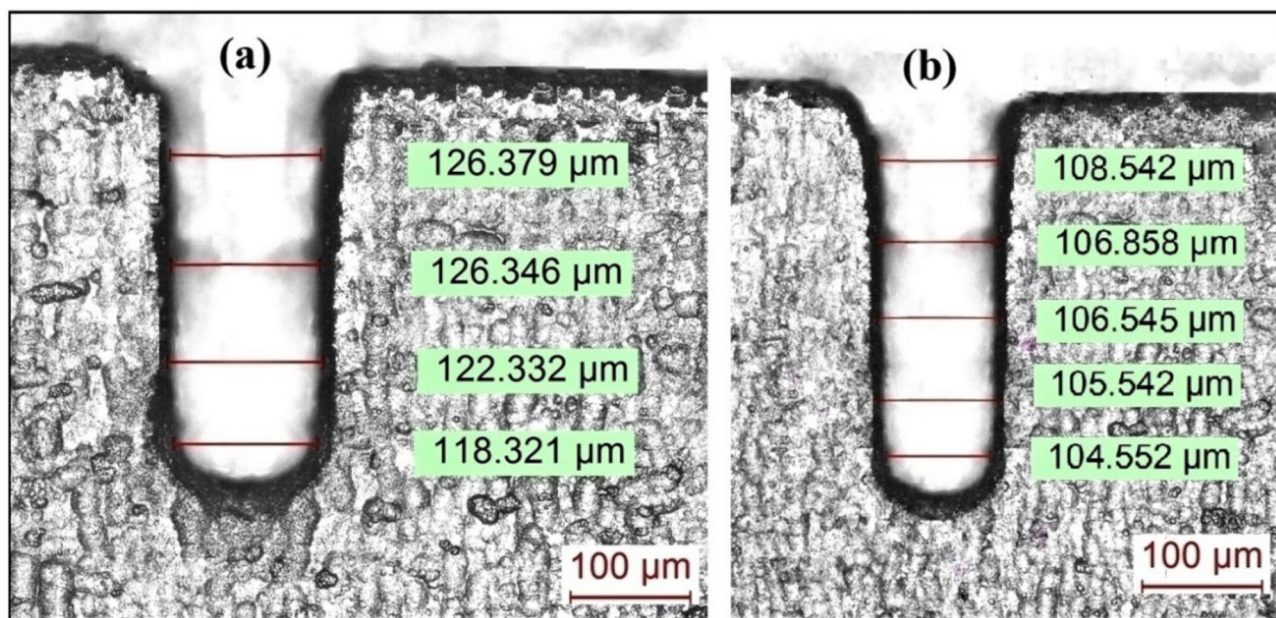


**Fig. 15** Fabricated microslits with **a** mixed ozonated 0.2 M $NaCl + 0.2$ M $NaNO_3$ electrolyte and **b** mixed ozonated 0.2 M $NaCl + 0.2$ M $NaNO_3 + 0.2$ M EDTA electrolyte
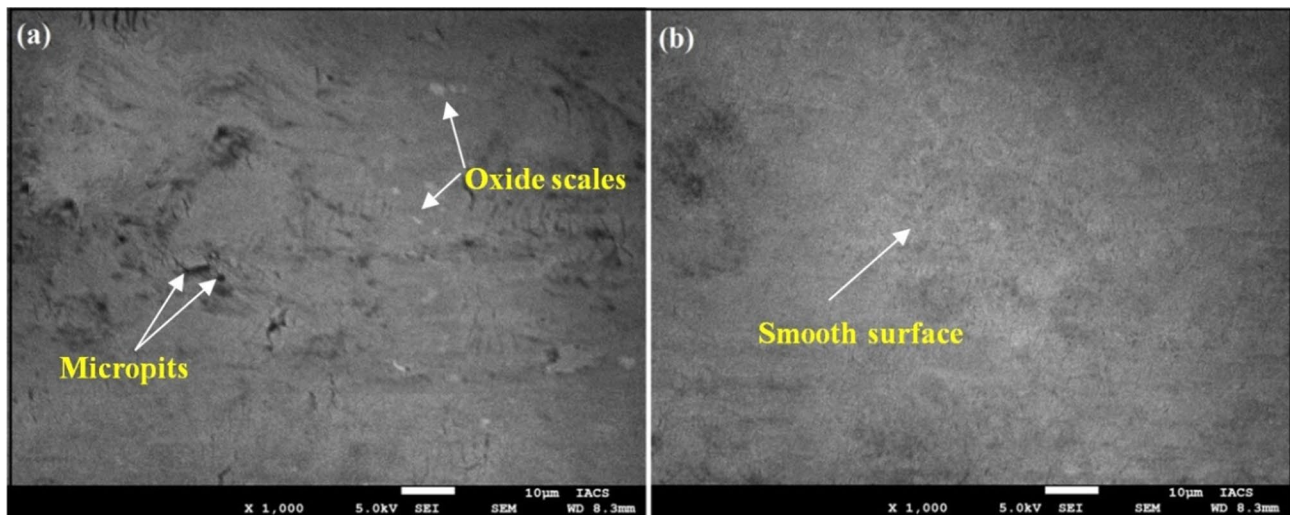
**Fig. 16** FESEM microstructure of machined microgroove surfaces at **a** ozonated 0.2 M NaCl + 0.2 M NaNO$_3$ and **b** mixed ozonated 0.2 M NaCl + 0.2 M NaNO$_3$ + 0.2 M EDTA electrolyte

with the measured average surface roughness values (Ra) of 0.1239 μm are shown in Fig. 16. It can be seen that the machined microslit surface obtained with 0.2 M ozonated 0.2 M NaCl + 0.2 M NaNO$_3$ has few micropits and very small oxide scales. These micro pits form as the electrolyte temperature rises with increasing current density in the machining zone. However, the machined surface condition with mixed ozonated 0.2 M NaCl + 0.2 M NaNO$_3$ + 0.2 M EDTA is smoother with negligible defects on the surface. Hence, it has been proven that the application of EDTA with mixed NaCl + NaNO$_3$ electrolytes in ozonated condition improves the machining accuracy and surface finish of fabricated nitinol shape memory alloy microfeatures during wire electrochemical machining.

## Conclusions

This research work demonstrates the significance of understanding the effects of various electrolytes with different mixed and ozonated conditions in order to accomplish a satisfactory machining operation for nitinol SMA. Furthermore, dimensional characteristics and surface topography of SMA machined surfaces were performed using FESEM, EDS, and CCI. The research findings can be summarized as follows:

(i) In the case of NaBr, machining of microgroove fabrication was not successful due to non-uniform dissolution and due to formation of sticky sludge, depth of machining is also very shallow throughout the nitinol surface area, surface roughness (Ra) is also very high compared to both NaCl and NaNO$_3$

electrolytes, and the best possible dissolution was obtained in the case of aqueous 0.2 M NaNO$_3$ electrolyte with groove width of 123.30 μm and mean groove depth of 179.7 μm with a surface roughness Ra of 0.379 μm. Further, it increases with increase in concentrations for all these electrolytes

(ii) It is observed that the use of mixed aqueous 0.2 M NaCl + 0.2 M NaNO$_3$ in combination with 0.2 M EDTA that forms soluble complexes with titanium ions to minimize the production of TiO$_2$ layers in these electrolytes. Hence, the combination of these electrolytes improved the performance of machining in terms of accuracy and surface finish for machining of nitinol compared to simple individual aqueous electrolyte solution. The mean depth of machined microgroove with mixed 0.2 M NaCl + 0.2 M NaNO$_3$ + 0.2 M EDTA electrolyte has been improved to 232.9 μm, which is more as compared to mean depth of mixed 0.2 M NaCl + 0.2 M NaNO$_3$ electrolyte. As far as width overcut is concerned in both these combination of electrolyte, there is no remarkable difference. Also, the average surface roughness value Ra is 0.2790 μm in this electrolyte, which is better than mixed 0.2 M NaCl + 0.2 M NaNO$_3$ shows improvement in the machining process

(iii) It shows that ozonated mixed 0.2 M NaCl + 0.2 M NaNO$_3$ + 0.2 M EDTA electrolyte has been proven as the most suitable electrolyte combination to achieve better dimensional characteristics and surface finish of nitinol during wire electrochemical machining. The EDS findings reveal that oxygen present on the machined surface has lower value, implying that the nitinol surface has no more passivity in the

electrolyte solution containing EDTA under ozonated condition compared with other non-ozonated conditions. The average groove width is 118.35 μm, 115.365 μm, 112.68 μm, and 105.86 μm; mean depth is 188.7 μm, 232.9 μm, 245.9 μm, and 264.6 μm; and the surface roughness (Ra) of the machined surface achieved was 0.3333 μm, 0.2790 μm, 0.2258 μm, and 0.1346 μm with mixed 0.2 M $NaCl+0.2$ M $NaNO_3$, mixed 0.2 M $NaCl+0.2$ M $NaNO_3+0.2$ M EDTA, ozonated mixed 0.2 M $NaCl+0.2$ M $NaNO_3$, and ozonated mixed 0.2 M $NaCl+0.2$ M $NaNO_3+0.2$ M EDTA electrolytes, respectively

(iv) The microslit has been fabricated at 5 V pulse voltage, 45% duty ratio, and 1.4 μm/s using ozonated mixed 0.2 M $NaCl+0.2$ M $NaNO_3$ and 0.2 M $NaCl+0.2$ M $NaNO_3+0.2$ M EDTA aqueous electrolyte solutions shows proper homogeneity with minimum average slit width of 106.40 μm and surface roughness (Ra) of 0.1261 μm. It can be seen that the machined microslit surface obtained with ozonated 0.2 M $NaCl+0.2$ M $NaNO_3$ has few micropits and very small oxide scales. These micropits form as the electrolyte temperature rises with increasing current density in the machining zone. However, the machined surface condition with mixed 0.2 M ozonated 0.2 M $NaCl+0.2$ M $NaNO_3+0.2$ M EDTA is smoother with negligible defects on the surface. Hence, it has been proven that the application of EDTA with mixed aqueous ozonated 0.2 M $NaCl+0.2$ M $NaNO_3$ electrolytes to improve machining accuracy and surface finish of fabricated nitinol shape memory alloy microfeatures during wire electrochemical machining

The scope of this investigation is to know the effect of different ozonated and non-ozonated neutral aqueous electrolytes, i.e., NaBr, NaCl, and $NaNO_3$, and addition of EDTA as a complexing agent are most suitable electrolytes during WECM of nitinol shape memory alloy. It has been revealed that the better results in terms of overall improvement in dimensional characteristics and surface quality during micromachining of difficult to cut nitinol shape memory alloy using wire electrochemical machining have been obtained with the application of mixed ozonated aqueous electrolytes. The addition of EDTA in electrolytes enhanced the performance of machining in terms of surface finish of nitinol which has prime importance in biomedical and various advanced engineering applications. However, further in-depth research may be needed for performance enhancement of WECM using different mixed electrolytes in aqueous and non-aqueous conditions during fabrication of complex micro-features of nitinol shape memory alloy.

## References

1. Bhattacharyya B (2015) Electrochemical micromachining for nanofabrication. William Andrew applied science publishers, Imprint of Elsevier Inc., Massachusetts, USA, MEMS and nanotechnology
2. Das B, Parimanik SR, Mahapatra TR, Mishra D (2022) Machinability assessment of NiTinol shape memory alloy in electrochemical machining. Int J Mach Mach Mater 24:280
3. Mwangi JW, Nguyen LT, Bui VD, Berger T, Zeidler H, Schubert A (2019) Nitinol manufacturing and micromachining: a review of processes and their suitability in processing medical-grade nitinol. J Manuf Process 38:355–369
4. Li S, Zeng Y, Hang Y, Yang T (2019) Improving surface quality and machining efficiency of microgrooves by WECMM in $H_3PO_4$-$C_2H_5OH$ solution. J Electrochem Soc 166(16):E584–E593
5. Takashi M (2003) Pulse electrochemical etching of NiTi shape memory alloy in LiCl-ethanol electrolyte. J Surf Sci Soc Jpn 54:693–697
6. Ao S, Li K, Liu W, Qin X, Wang T, Dai Y (2020) Electrochemical micromachining of NiTi shape memory alloy with ethylene glycol–NaCl electrolyte containing ethanol. J Manuf Process 53:223–228
7. Sethi A, Acharya BR, Saha P (2022) Study of the electrochemical dissolution behavior of nitinol shape memory alloy in different electrolytes for micro-ECM process. Int J Adv Manuf Technol 121:7019–7035
8. Lee ES, Shin TH (2011) An evaluation of the machinability of nitinol shape memory alloy by electrochemical polishing. J Mech Sci Technol 25(963):6
9. Guo Y, Klink A, Fu C, Snyder J (2013) Machinability and surface integrity of nitinol shape memory alloy. CIRP Ann Manuf Technol 62:83–86
10. Ma X-Z, Li Z, Guo HC, Yu L, Jing T (2007) Electrochemical micromachining of nitinol by confined-etchant-layer technique. Electrochemical Acta 52:4191–4196
11. Saxena KK, Qian J, Reynaerts D (2018) A review on process capabilities of electrochemical micromachining and its hybrid variants. Int J Mach Tools Manuf 127:28–56
12. Lopes NIDA, Silva LÁDO, Santos LDA, Buono VTL (2017) Surface characterization of NiTi superelastic and shape memory alloys after electrolytic polishing. Mater Res 20(Suppl. 2):572–579
13. MouliPrasanth B, Hariharan P (2021) Evaluation of 3D surface roughness in electrochemical micromachining of nitinol. Surf Topogr Metrol Prop 9:045012
14. Hang Z, Fang X, Zeng Y, Zhu D (2022) Wire electrochemical trimming the recast layer on Ren´e 88DT for aero-engine applications. Electrochemical Acta 418:140372
15. Lee ES, Shin TH, Kim BK, Baek SY (2010) Investigation of short pulse electrochemical machining for groove process on Ni-Ti shape memory alloy. Int J Precis Eng Manuf 11(1):113–118
16. Sharma V, Patel DS, Jain VK, Rajkumar J (2020) Wire electrochemical micromachining: an overview. Int J Mach Tools Manuf 155:103579
17. Besekar N, Bhattacharyya B (2022) Wire electrode insulation method for stray current and overcut reduction during WECM—a novel approach. J Adv Manuf Technol 123:3917–3942
18. Sethi A, Acharya BR, Saha P (2022) Electrochemical dissolution of WC-Co micro-tool in micro-WECM using an eco-friendly citric acid mixed $NaNO_3$ electrolyte. J Electrochem Soc 169:033503

19. Xu K, Zeng Y, Li P, Zhu D (2015) Study of surface roughness in wire electrochemical micro machining. J Mater Process Tech 222:103–109

20. Tak M, Reddy VS, Mishra A, Mote RG (2018) Investigation of pulsed electrochemical micro-drilling on titanium alloy in the presence of complexing agent in electrolyte. J Micromanuf 1(2):142–153

21. Jiang K, Wu X, Lei J, Wu Z, Wu W, Li W, Diao D (2018) Vibration-assisted wire electrochemical micromachining with a suspension of B4C particles in the electrolyte. J Adv Manuf Technol 97:3565–3574

22. Kalaimathi M, Venkatachalam G, Sivakumar M, Ayyappan S (2017) Experimental investigation on the suitability of ozonated electrolyte in travelling-wire electrochemical machining. J Braz Soc Mech Sci Eng 39:4589–4599

23. Anasane S, Bhattacharyya B (2016) Experimental investigation on suitability of electrolytes for electrochemical micromachining of titanium. Int J Adv Manuf Technol 86:2147–2160

24. Sethi A, Acharya BR, Saha P (2023) Parametric investigation of pulse frequency and microtool rotational speed for precise fabrication of microchannels on nitinol shape memory alloy through ECMM. Material Today Communications 36:106844

25. Besekar N, Bhattacharyya B (2022) Experimental investigation and characterization of NiTinol shape memory alloy during wire electrochemical machining. J Manuf Process 81:346–361

26. Ding R, Shang JX, Wang FH, Chen Y (2018) Electrochemical Pourbaix diagrams of Ni–Ti alloys from first- principles calculations and experimental aqueous states. Comput Mater Sci 143:431–438

27. Pichavant A, Provost V, Furst W, Hochepied JF (2019) Determination of the temperature dependence of (IV) hydrolysis and complexation constants in aqueous sulphuric and chlorhydric solutions, J Chem. Thermodynamics 131:184–191

28. Jinxing J, Cooper WC (1996) Nickel speciation in aqueous chloride solution. Electrochim Acta 41(9):1549–1560

29. Sreekumar NV, Bhat NG, Narayana B (2003) Selective complexometric determination of titanium(IV) using sodium potassium tartrate or ascorbic acid as masking agent. Mikrochim Acta 141:29–33